CORRECTION OF AB VARIANT G_{M2} GANGLIOSIDOSES USING AAV9 VIRAL VECTOR GENE THERAPY IN A MOUSE MODEL

by

Meera B. Vyas

A thesis submitted to the Department of Neuroscience

In conformity with the requirements for

Degree of Master of Science

Queen's University

Kingston, Ontario, Canada

(July 2019)

Abstract

G_{M2} Gangliosidoses are a group of neurodegenerative diseases affecting the brain. In humans, these diseases are characterized by rapid neurological deterioration and death before 4-years of age. G_{M2} gangliosides are normally degraded in a cell's lysosomes through the action of three gene products, *HEXA*, *HEXB*, and *GM2A*. A defect in any one of these genes can result in a deficiency of Hexosaminidase A (HexA) enzyme activity, which then cannot breakdown G_{M2} gangliosides. The rarest form of these diseases, the AB-variant (AB- G_{M2}), is characterized by a mutation in the *GM2A* gene encoding the GM2-activator protein (GM2AP), which is a required co-factor for the HexA protein. The aim of this study is to give a one-time treatment of single stranded (ss) AAV9/*GM2A* viral vector therapy at a dose of 1×10^{14} vector genomes per kilogram of mouse and to see at least biochemical reduction in G_{M2} ganglioside storage in both the short- and long-term treated cohorts. ssAAV9/*GM2A* plasmid was created and tested *in vitro* on a GM2AP-deficient patient cell line to confirm the expression of the protein using Western Blot analysis. Later, treatments were given to 1-day old pups via the superficial temporal vein, as well as 6-week old adult mice via tail vein, to correct AB- G_{M2}. These mice underwent monthly behavioural testing, as well as biochemical and molecular analysis performed at 20- and 60-week end-points. We hypothesized that an optimized ssAAV9/*GM2A* treatment can correct the gene mutation as well as phenotype of AB- G_{M2} in mice. Biochemical data for both end-points showed reduction in G_{M2} gangliosides storage in the treated cohorts compared to the vehicle cohorts for both the neonatal and adult treated cohorts. Behavioural data for the 20- and 60-week end-points, as well as the neonatal treated and adult treated mice, showed the treated cohorts inconsistently outperformed the vehicle cohorts. Almost uniform biodistribution of the hGM2AP vector was also seen across the rostral section, caudal section, mid-section and liver. This proof of concept

study is a step forward towards the development of a therapeutic approach for AB-G_{M2} and towards our goal of human clinical gene therapy trials.

Contribution Statement

This study was designed, directed and coordinated by Meera Vyas, and Dr. Jagdeep Walia. Dr. Jagdeep Walia., as the principal investigator, provided conceptual and technical guidance for all aspects of the project. Dr. Harriet Feilotter, Dr. Andrew Winterborn and Dr. Stephen Scott also provided revisions and guidance for the project. Gene synthesis was done by Biobasic, a Toronto based research laboratory. The viral vector was constructed by a core vector facility at the University of North Carolina. Final western blot completed by Chris Richmond (Funk lab, MSc). 40-60 week behavioural testing for long-term cohort completed by Natalie Deschenes (Walia Lab, PhD Candidate). qT-PCR performed and analyzed by Zhilin Chen (Walia Lab, Technician). Microtome sectioning and histology staining completed by Karlaina Osmon (Walia Lab, PhD Candidate). Histology slides completed by Shakeel Virk and Lee Boudreau (Richardson Labs).

Acknowledgements

There is such a large group of people who have continued to support me throughout my academic career. I would like to firstly thank Dr. Jagdeep Walia for all of his guidance and continued support throughout my Master's journey. I would like to thank my committee members Dr. Andrew Winterborn and Dr. Harriet Feilotter; for being supportive figures and available for guidance when needed. I would also like to thank Dr. Colin Funk for allowing me to use his lab space and learn a great deal from his lab members as well.

I would not have been able to complete this Masters without the help of the laboratory technicians in both the Walia Lab and the Funk Lab. Not only were they greatly knowledgeable on many of the biochemical analyses and optimizations, and were readily available to come to my rescue; but they had a solid work ethic, which I admired and learnt a great deal from. I would like to thank Zhilin Chen, Patrick Thompson, and Laurel Ballantyne.

I would like to extend a great thank you to all of my laboratory mates in both the Walia lab and Funk lab. Karlaina, you did a wonderful job orienting me to the laboratory environment, which was such an unfamiliar territory for me initially. I learned a great deal from you and you became a good friend of mine through my research endeavours. I'm not sure if you realize how big of an impact you had on my experience as a Master's student; but I will continue to remember many of our lab days fondly. Evan, I would like to thank you for your witty comments and your ability to lighten any situation. Imtiaz, we were both so new to basic science research and I have grown to build a wonderful friendship out of our Master's journey. You have allowed me to appreciate so much and I have tried to emulate your work ethic to this day. Shal, you were a great 499 student and we were so happy to have you come to our lab to do a Master's thesis. Not only did we work hard together, but also we shared a lot of good laughs and you definitely brought out my goofy side. Natalie, thank you for continuing with my behavioural work while I've been going through residency. I cannot imagine how I would have balanced both important tasks at once. Chris, I knew I could always count on you to be smiling and make some outlandish remark to make me laugh even if I was having a tough day. I am also greatly thankful for how you managed to produce a Western blot that I tried to perfect for several months on end with minimal success. I would like to also thank Angie Sin, and Xinghi who always graciously provided me with extra clarification and came to my aid whether it be for optimizing an assay, a Western blot gone wrong or just advice on life.

Most importantly, I would like to thank my family. My parents are a wonderful example of how hard work pays off and continue to support me throughout my life, especially through my academic career. My mother always told me everything happens for a reason and not to dwell on anything for too long; and my father taught me how to live in the attitude of gratitude. There were many days where I would come home disheartened from a failed assay or a tough day with mouse work and they would always be ready to lift my spirits. I would like to thank my younger sister, Aarti, and my younger brother, Bhavik, who have always cheered me on through all of my endeavours and who continue to be a wonderful support system. I would also like to thank my fiancé, Rickul, who has been with me throughout my Master's journey and my newest endeavor as a pediatric resident. He has been my voice of reason, always telling me to persevere and to charge on until the finish line, thank you for always asking about my day and caring so much.

Table of Contents

List of Tables

List of Figures

List of Abbreviations

AAV – Adeno-Associated Virus

AB- G_{M2} - AB variant G_{M2} gangliosidoses

ANOVA – Analysis of Variance

BBB – Blood brain barrier

BC – Biochemistry

CB – Caudal brain

CNS – Central nervous system

DNA – Deoxyribonucleic acid

dsDNA – Double stranded DNA

GFP – Green fluorescent protein

GM2A(P) – GM2 activator (protein)

KO – Knock out

Hex – Hexosaminidase

HexA – β-Hexosaminidase A isozyme

HexB – β-Hexosaminidase B isozyme

HexS – B-Hexosaminidase S isozyme

Hist – Histology

HSCT/BMT – Hematopoeitic stem cell therapy/Bone marrow transplant

LSD – Lysosomal storage disease

MB – Mid-section of brain

OFT – Open field test

PBS – Phosphate buffered saline

PCR – Polymerase chain reaction

qPCR – Quantitative real-time polymerase chain reaction

rAAV – Recombinant Adeno-associated virus

RB – Rostral brain

RR – Rotarod

RPM – End rotations per minute

SD – Sandhoff Disease

scAAV – Self complimentary Adeno-associated virus

ssDNA – Single stranded DNA

SRT – Substrate reduction therapy

TSD – Tay-Sachs disease

TBS – Tris-buffered saline

Chapter 1

Introduction

1.1 G_{M2} Gangliosidoses and AB-G_{M2}

G_{M2} Gangliosidoses are a set of neurodegenerative diseases that affect the brain. The three known types are Tay-Sachs, Sandhoff and G_{M2} Ganglioside AB variant (AB-G_{M2}). This group of diseases have an autosomal recessive inheritance pattern and are caused by mutations in genes which encode for particular enzymes or factors that break down G_{M2} Gangliosides (Figure 1). Essentially, this leads to a toxic build-up of G_{M2} gangliosides in the body, with the highest concentrations seen in the brain.

G_{M2} Gangliosidoses encompasses three diseases where the hallmark is the inability to catabolize G_{M2} gangliosides into G_{M3}, which occurs due to mutations in any component of the HEXA-GM2AP complex. The HEXA protein is a heterodimer comprised of two subunits, the alpha and beta, coded by the *HEXA* and *HEXB* genes, respectively (Figure 1). The HEXA protein then complexes with the GM2A protein cofactor (GM2AP), coded by the *GM2A* gene, in order to catabolize G_{M2} gangliosides (Figure 2). Tay-Sachs disease (TSD) occurs when there is a mutation of the *HEXA* gene, leading to malfunctioning alpha-subunit, resulting in a large build-up of the G_{M2} ganglioside glycolipids within the neurons of the brain and spinal cord (Sandhoff 1977; Okada and O'Brien 1969). Sandhoff disease (SD) occurs when there is a mutation in the *HEXB* gene, leading to abnormal beta subunit and thus causing deficiency of the HEXA protein, causing neurotoxic accumulation of G_{M2} gangliosides (Sandhoff 1977). Lastly, the AB-variant of G_{M2} Gangliosidosis (AB- G_{M2}) occurs due to mutations in the *GM2A* gene. *HEXA* and *HEXB* genes are at normal levels in AB- G_{M2} (Gravel et al., 2014). When large amounts of gangliosides are stored within the brain and spinal cord, this leads to neurological deterioration and in its severest infantile form, has the potential of causing death by the early age of 4 (Sandhoff et al., 2013). Of the three genetic deficiencies, TSD is the most commonly seen condition and AB- G_{M2} is the rarest seen condition (Mahuran, 1999).

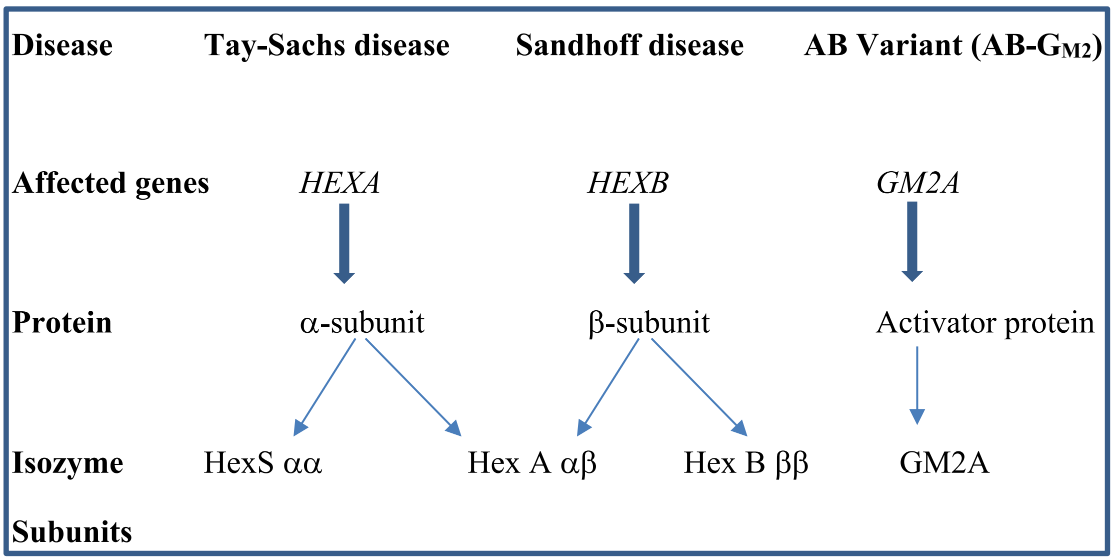

Figure 1. The G_{M2} Gangliosidoses. The disease along with the associated genes, proteins, isozyme subunits as well as accumulated substrates.

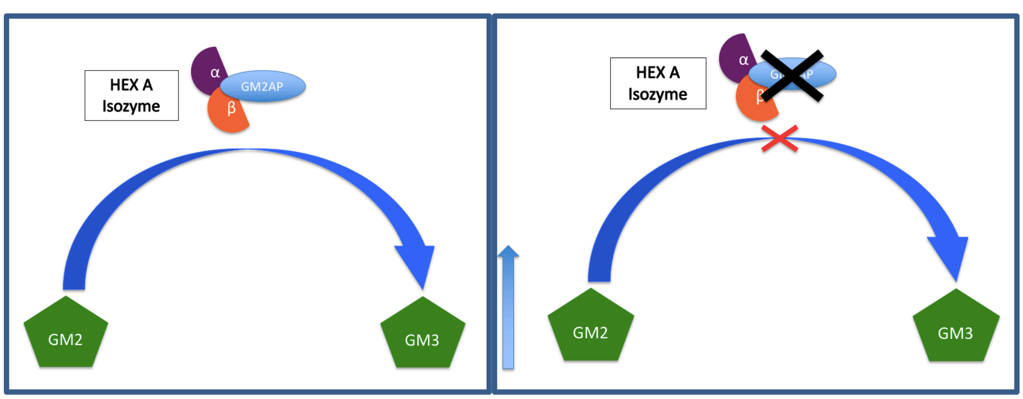

Figure 2. G_{M2} Ganglioside Metabolism & Build-Up

1.1.1 Epidemiology

It has been estimated that to date, there are fewer than ten confirmed cases of AB- G_{M2} by molecular analyses worldwide (Renaud & Brodsky 2016); however, the incidence could be higher due to under diagnosis and underreporting of this condition. Disease severity in terms of cognitive dysfunction, decreased motor skills, and problems with vision, are related to the level of enzyme deficiency, as well as the resultant ganglioside accumulation in the brain and spinal cord (Lawson and Martin 2016; Liu et al., 1997). The degree to which the enzyme loses its functionality also helps determine if the individual will present with an early- (infantile onset) versus late-stage (juvenile or adult onset) form of AB- G_{M2} (Liu et al., 1997).

1.1.2 Function of G_{M2} Activator Protein

GM2AP is a lysosomal protein that acts as a substrate-specific co-factor along with Hexosaminidase (HEXA) protein. The α/β heterodimer forms a complex with the GM2AP that allows for the breakdown of G_{M2} gangliosides into G_{M3} gangliosides (Mahuran 1998). GM2AP is located on chromosome 5q33.1. It is 193 amino acids in size, with a molecular mass of 20,838 Daltons.

Studies are beginning to reveal various alternative functions for the GM2AP. GM2AP has been shown to bind, solubilize and transport various lipid molecules, which include glycosphingolipids, gangliosides and phosphoacylglycerol between liposomes (Mahuran 1998). GM2AP has also been shown to have sphingolipid activator protein activity and can also be called saposin-3, as GM2AP belongs to the family of saposins (Werth et al., 2001). A study done by Yanai et al. in 2006 indicates that higher levels of glycosphingolipids have been seen in the aorta and serum of humans suffering from atherosclerosis and in animal models of atherosclerosis, implying that GM2AP has a contributing role in the progression of atherosclerosis (Yanai et al., 2006).

Another study investigated the structural basis of GM2AP's ability to bind to phospholipids (Mathias et al., 2009; Wright et al., 2005). Due to the large binding pocket, GM2AP is able to adhere to many single-chain phospholipids as well as fatty acids (Mathias et al., 2009; Wright et al., 2005). This study also demonstrated that GM2AP was able to hydrolytically modify phospholipids (Wright et al., 2005). These combined effects of GM2AP could have significant meaning for lipid metabolism as well as cellular signaling (Wright et al., 2005). Hydrolase activity may also explain GM2AP's ability to inhibit the inflammatory processes otherwise initiated by platelet activating factor-induced disease processes, as these may occur secondary to an enzymatic reaction modifying platelet activating factor (PAF) to a nontoxic lyso-PAF (Rigat et al., 2009, Wright et al., 2005).

Studies have also demonstrated that GM2AP may be a useful biomarker to monitor the progression and diagnosis of lung cancer (Potprommanee et al., 2013). In each of the subtypes of lung cancer patients, GM2AP was significantly increased in comparison to healthy controls, proposing an association of GM2AP to tumor-associated gangliosides (Potprommanee et al., 2013). Another study evaluated various secretomes as potential candidates for cancer markers and showed that a higher amount of GM2AP was found in the plasma of individuals who suffered from estrogen receptor negative breast cancer (Shin et al., 2016).

1.1.3 Pathophysiology

Glycosphingolipids are essential for the development of eukaryotic organisms (Sandhoff & Kolter 2003) and play a role in cell adhesion as well as the regulation of membrane proteins (Varki, 1993; Yang et al., 1996). Activator proteins are one of the many components required to break down sphingolipids (Kolter and Sandhoff 2005). The GM2AP is required as a cofactor in the *in vivo* degradation of G_{M2} gangliosides by β-hexosaminidase A (Conzelmann & Sandhoff 1979). Gangliosides are made up of a ceramide backbone attached to oligosaccharide side chains, with or without the addition of sialic acid (Sandhoff & Kolter 2003). Gangliosides are catabolized through a series of hydrolytic processes that are controlled by particular lysosomal enzymes (Lawson & Martin 2016). The AB-G_{M2} is defined as an inherited mutation in this particular GM2AP. In a normal functioning system the *HEX* genes (*HEXA* and *HEXB*), code for protein subunits (α and β) (Liu et al., 1997). The subunits then dimerize and are able to create three β-hexosaminidase isozymes, A (α/β), B (β/β), and lastly S (α/α) (Sandhoff & Conzelmann 1978). The GM2AP cofactor then complexes with the HEXA protein to breakdown G_{M2} gangliosides. In AB-G_{M2} there are normal levels of the HEX isozymes, but there is malfunctioning of the GM2AP co-factor. The resultant accumulation of G_{M2} ganglioside occurs commonly in neuronal cells (Sandhoff & Kolter 2006).

1.1.4 Clinical Presentation of AB-G_{M2}

The clinical presentation of AB- G_{M2} is similar in its infantile form to TSD (Ferreira & Gahl 2017). There is normal early infant development; up to approximately 6 months of age, and this is followed by developmental delay and regression (Martin et al., 2005). The infant begins to demonstrate progressive weakness and neuromuscular deterioration, exaggerated startle response, vision loss along with a cherry red spot in the fundus of the retina, dysphagia, seizure activity and macrocephaly (Martin et al., 2005). To date almost all of the individuals who have presented with AB-G_{M2} have demonstrated a classic infantile clinical phenotype (Renaud & Brodsky 2016).

1.1.5 Current Animal Models

Murine model

The mouse model for AB- G_{M2} has been generated through targeted gene disruption (Liu et al., 1997). The GM2AP exon 3, intron 3 and a portion of exon 4 in 129S2/SvPas-derived D3 embryonic stem (ES) cells, was disrupted using a targeting vector containing neomycin resistance and Herpes simplex virus thymidine kinase genes (Liu et al., 1997). The ES cells that were correctly targeted were then injected into C57BL/6 blastocysts (Liu et al., 1997). This mouse model has a normal life span, but showed cerebellar pathology; due to G_{M2} ganglioside build-up, and motor deficiencies with defects in balance and coordination; which are usually evident after 4-months of age in the mouse model (Liu et al., 1997). Neuronal storage is found predominantly in the piriform area, entorhinal cortex, amygdala, hypothalamic nuclei, cerebellum and pyramidal neurons of the middle cerebral cortical layer (Liu et al., 1997, Martin et al., 2005). It is an intermediate phenotype especially for survival in comparison to the TSD and SD murine model of G_{M2} gangliosidoses, with the TSD mouse model showing a normal life span and SD mouse model having survival to 16-17 weeks. Thus, this model mimics adult onset human disease phenotypically; which could be a limitation of the mouse model. The reason behind the difference in disease severity in the mouse model compared to humans is due to an alternative degradation (via sialidase) pathway that is present in mice; which is not present in humans (Bertoni et al., 1999; Yuziuk et al., 1998). This is what creates the difference in survival in mice compared to humans; as the mouse model shows a normal life span similar to a heterozygous mouse. Humans have a significantly decreased survival span, with survival up to the approximate age of 4 years and do not have the alternative pathway. In humans, HexA degrades G_{M2} gangliosides, which is why TSD (α subunit deficiency) produces such an impressive G_{M2} ganglioside accumulation (Lawson & Martin 2016).

The advantages of using a mouse model for such a disease state and for testing various therapeutic strategies would be: the quick turn-around time for analyzing successful or failed approaches; the short time period that is able to produce large numbers of animals for testing and the ease of breeding and housing the animals in a relatively small animal facility. Cost is also much more effective in using a small animal model for testing.

Feline model (one case report, not bred for research)

The feline model was discovered and characterized in a male orange tabby domestic shorthair cat (Martin et al., 2005). Clinical symptomology for the feline model begins at approximately 14 months of age (Martin et al., 2005). These clinical signs include an exaggerated startle response and difficulty with motor coordination, as well as ataxia and intention tremors (Martin et al., 2005). With progression of the disease, cats also have difficulty in ambulation and eating (Martin et al., 2005). There are also central nervous system manifestations that are seen showing swollen neurons, membranous cytoplasmic bodies and a higher content of sialic acid as well as storage of G_{M2} gangliosides (Martin et al., 2005).

Canine model (one case report, not bred for research)

The canine model was found in a Japanese Spaniel dog (Lawson & Martin 2016; Martin et al., 2005). The canine model shows disease onset of GM2A deficiency at 18 months and there is gradual neurological deterioration showing tremor and ataxia (Lawson & Martin 2016). There is a global accumulation of G_{M2} gangliosides, in contrast to the mouse model in which accumulation is limited to certain areas of the brain (Lawson & Martin 2016; Liu et al., 1997).

1.1.6 Current Treatment

Currently there is no specific therapy for G_{M2} Gangliosidoses, including AB- G_{M2}. In many rare heritable diseases, early diagnosis is key for treatment and prognostic outcomes. However, even with the ability to provide an early diagnosis for some affected infants, there are currently no specific gold standard or curative treatments approved for G_{M2} Gangliosidoses. Still, there are many therapeutic approaches that are currently under investigation in animal models and cell-culture models of G_{M2} Gangliosidoses and various other monogenic disease states.

Hematopoietic Stem Cell Therapy and Bone Marrow Transplantation (HSCT/BMT)

Hypothetically allogenic HSCT/BMT may work for AB- G_{M2} if the therapy is implemented early; as this would give less time for G_{M2} ganglioside build up and may provide some restoration of GM2AP. HSCT/BMT works by an influx of healthy donor cells into an enzyme-deficient bone marrow in hopes of restoring some enzyme activity (Krivit et al., 1999; Macauley 2016; Malatack et al., 2003, Platt & Lachmann 2009). There has been some degree of success in using this method in other lysosomal storage disorders like Hurler disease. HSCT/BMT has had some success in restoring deficient enzyme activity, but this has a great deal to do with the timing of when the therapy is provided and how acutely the disease has progressed (Boelens 2006; Li & Sands 2014). There has been some success in treating patients before symptom onset or milder forms of the disease (Macauley 2016).

Substrate Reduction Therapy (SRT)

SRT works by inhibiting the synthesis of compounds that are not degradable by the patient's own cells, due to deficient enzymatic activity (Clark & Hollak 2015; Hollak & Wijburg 2014; Platt et al., 2009). Hypothetically SRT may work for AB- G_{M2} as well if the therapy is implemented early, as build-up of G_{M2} gangliosides would be minimal at birth and SRT may be able to inhibit the synthesis of new G_{M2} gangliosides. However, this therapy may be limited as the accumulation of G_{M2} gangliosides may be faster than the ability to inhibit synthesis of gangliosides. This therapy has shown some effectiveness in animal models of various diseases (Cox et al., 2000; Gabig-Ciminska et al., 2015; Hawkins-Salsbury et al., 2011). In terms of G_{M2} Gangliosidoses, SRT reduces the synthesis of gangliosides including G_{M2}. In murine models of TSD and SD, (miglustat) Zavesca is able to decrease the amount of gangliosides that accumulate in the brain and spinal cord (Macauley 2016). This is done by inhibiting glucosylceramide synthase (Maegawa et al., 2009). In Sandhoff mice that were treated with Zavesca, if the treatment was given before symptoms developed, there was an increase in life expectancy by approximately 40% (Jeyakumar et al., 1999). There was also halting of disease progression seen in two infantile Tay-Sachs patients who had been treated with Zavesca after they began having clinical symptoms (Macauley 2016). The most common side effects of miglustat include diarrhea, flatulence and abdominal pain (Jarnes Utz et al., 2017). The benefits of using SRT as opposed to a biologic is that it bypasses issues such as immune response that impact ERT, as well as graft-versus-host disease that can occur with HSCT/BMT or issues of immunogenicity that can occur with gene therapy (Macauley 2016). SRT has not been tested for AB-$_{GM2}$.

Chapter 2

Literature Review: A Look at AAV Vectors and Gene Therapy

2.1 Viral Vectors

All viral vectors have functions that are in common, which let the vectors become useful as potential therapeutic delivery vectors. Important criteria that should be met in order for a viral vector to be efficient would be the vector's ability to generate at a stable rate and have targeted delivery (Thomas et al., 2003). They need to have the ability to target delivery to a specific tissue or organ of interest, a term called tropism (Thomas et al., 2003). Finally, viral vectors need to be able to moderate gene delivery and express transgenes without causing adverse secondary responses (Thomas et al., 2003).

There are five main classes of viral vectors, which can be divided into two groups depending on whether their genomes are integrated into host cellular chromatin, such as onco-retroviruses and lentiviruses; or if their genomes remain in the cell nucleus primarily as extrachromosomal episomes, such as herpes viruses, AAVs, and adenoviruses (Kay et al., 2001) (Table 1). This division allows specific viral vectors to be used for particular applications. Non-integrating vectors allow for constant transgene expression in non-proliferating cells, but integrating vectors are used for stable genetic alteration in cells that are dividing and non-dividing (Kay et al., 2001).

Vector	Genetic Material	Packaging Capacity	Tropism	Inflammatory potential	Vector genome forms	Limitations	Advantages
Enveloped							
Retrovirus	RNA	8kb	Multiplying cells	Low	Integrated	Only affects multiplying cells and may have oncogenic potential	Stable gene transfer in dividing cells
Lentivirus	RNA	8kb	Extensive	Low	Integrated	May have oncogenic potential	Stable gene transfer in most tissues
Herpes Simplex Virus (HSV-1)	dsDNA	40kb	Neurons	High	Episomal	Inflammatory, temporary transgene expression in non-neuronal cells	Large packaging capacity; strong affinity for neurons
Non-enveloped							
AAV	ssDNA	<5kb	Extensive	Low	Episomal (>99%) Integrated (<1%)	Minimal packaging capacity	Non-inflammatory; non-pathogenic
Adenovirus	dsDNA	8kb	Extensive	High	Episomal	Strong inflammatory response	Very productive transduction of most tissues

Table 1. Classic Viral Vector Groups used in Gene Therapy.
Table adapted from (Osmon et al., 2016; Thomas et al., 2003)

2.1.1 AAV serotypes

There are many serotypes of AAV that have been established, with AAV2 being the most commonly used (Hardcastle et al., 2018; McCown 2011). The differences in the serotypes stem from their abilities to infect different cells -tropisms, to target various organs (McCown 2011).

The table below (Table 2) summarizes the various tropisms of AAV serotypes and depicts the best serotype to use for efficient gene transduction in a particular organ or tissue.

Organ/Tissue	Ideal Serotype
CNS	AAV1, AAV2, AAV4, AAV5, AAV8, AAV9
Heart	AAV1, AAV8, AAV9
Kidney	AAV2
Liver	AAV7, AAV8, AAV9
Lung	AAV4, AAV5, AAV6, AAV9
Pancreas	AAV8
Skeletal Muscle	AAV1, AAV6, AAV7, AAV8, AAV9

Table 2. AAV Serotypes. **Adapted from Addgene.** Different serotypes have different tropisms for different tissues.

2.1.2 The Adeno-associated Virus: A Deeper Look

There are many advantages to using recombinant adeno-associated viral (rAAV) vectors in gene therapy as compared to other viral vectors. rAAVs are nonpathogenic, do not replicate and are able to transduce dividing and non-dividing cells (Coura and Nardi 2007). AAV vectors only integrate approximately 1% of the time and therefore are safer to use, compared to other vectors which have a higher integration rate (Gruenert et al., 2016). There are a number of cell types and tissues that AAV is able to transduce, including the liver, lung, muscle, bone marrow as well as the CNS (Lo et al., 1999).

2.1.3 Advantages and Disadvantages of AAV Vectors

The advantages of AAV viral vectors include the following: (1) lack of pathogenicity and lack of immunogenicity along with heat stability; (2) retention of approximately 300 nucleotides worth of viral sequence, as this decreases the risk of recombining with wild-type virus; (3) extensive host and cell tropism with the ability to infect both dividing and non-dividing cells *in vivo* and *in vitro* (Coura and Nardi 2007; Wright et al., 2003).

Advantages of AAV9, in particular, include its unique ability to cross the blood-brain barrier (BBB). This allows the vector to infect cells of the CNS which include primary neurons (Merkel et al., 2017). In various animal models, AAV9 has also been shown to effectively deliver genes to skeletal and cardiac muscles (Wang et al., 2014).

The disadvantages of ssAAV viral vectors include the following: (1) limitation of size, which does not allow for insertion of large gene expression cassettes; >5kb; (2) slow start to express genes, which is secondary to the rate limiting step of having to convert ssDNA to dsDNA before initiating gene expression (Coura and Nardi 2007).

AAV viral vectors have been shown to have relatively low immunogenicity in comparison to other viruses, such as adenovirus (Naso et al., 2017). However, the capsid protein, along with the nucleic acid sequence delivered are able to activate different areas of the immune system. An added complication is the fact that many people have already been exposed to AAV. This means they have already created an immune response to what they were previously exposed to; thus creating a pre-existing adaptive response. Local or systemic administration of the virus will be seen as a foreign protein, and so the body's adaptive immune system would attempt to remove it (Naso et al., 2017).

The use of an AAV viral vector for gene delivery currently appears to be the most promising system. It is the most utilized viral vector in therapeutic research today for monogenic diseases.

2.1.4 Single Stranded Adeno-associated Virus or Self-Complementary Adeno-associated Virus?

The genome of an AAV vector is packaged as linear ssDNA (Gruenert 2016). The ssAAV genome is approximately 4.7 kb in length (Gruenert 2016). After infection into the target cell, ssDNA needs to be converted into double-stranded (ds) DNA in order for gene expression to occur. The time required for this conversion serves to be the rate-limiting step for efficient transduction when utilizing ssAAV gene therapy for disease treatment (Ferrari et al., 1996; Fisher et al., 1996; McCarty 2008). This rate limiting step can be circumvented by using self-complementary (sc) AAV vectors as there is a dimeric inverted repeat genome within the AAV that allows for the vector to fold into dsDNA (McCarty 2008). One consequence of using scAAV is the ability of scAAV to only carry half of the ssAAV's coding capacity (~2.3kb) (McCarty 2001). However, scAAV is able to transduce a higher number of cells at the same dose as ssAAV (McCarty 2008).

2.2 Gene Therapy

History of Gene Therapy

Gene therapy can be divided into two categories being: germ line therapy and somatic gene therapy (Wirth et al., 2013). In somatic gene therapy there is insertion of genetic material into a target cell that is not passed to future generations. In germ line gene therapy, these gene effects are passed on to future generations because these mutations occur in reproductive cells (Wirth et al., 2013).

The first gene therapy clinical trial was done in 1990 in adenosine deaminase deficiency (ADA-SCID) patients, which is a monogenetic disease that results in extensive immunodeficiency (Wirth et al., 2013). These studies did not produce the expected results of successfully treating the disease process, but the interest in gene therapy was increasing; until the death of 18-year old Jesse Gelsinger (Blaese et al., 1995; Wirth et al., 2013). Mr. Gelsinger took part in a gene therapy clinical trial at the University of Pennsylvania (Stolberg, 1999). Jesse had a partial deficiency of ornithine transcarbamylase (OTC), for which he was given a high dose of the adenoviral vector based OTC gene therapy treatment, and his immune system showed an immediate response to a high dose of adenovirus that was administered (Stolberg, 1999). Consequently, Jesse died after four days secondary to disseminated intravascular coagulation and multi-organ failure (Stolberg, 1999). His death halted many clinical trials to provide an opportunity to refine the methods and safety of the gene delivery methods.

The field of gene therapy has progressed in the past 20 years and has made great progress. Currently, 65% of all clinical gene therapy trials conducted worldwide are being used to treat cancer (Ginn et al., 2017). The second and third most common diseases treated by gene therapy clinical trials are monogenic (11.1%) and infectious diseases (7%) (Ginn et al., 2017). The most commonly used viral vectors in these conditions have been adenoviral, retroviral and naked plasmids (Wirth et al., 2013).

2.2.1 Safety and Efficacy of Gene therapy

Immune response

One of the biggest hurdles facing gene therapy is the immune response that may be activated in response to vectors and/or new transgene products that the body may recognize as foreign (Kafri et al., 1998; Thomas et al., 2001). Adenoviral vectors are known to activate multiple components of the immune response. When dealing with drug-induced toxicities, the vector dose plays a large role in the degree of harmful immune-mediated and inflammatory responses that the viral vectors may produce (Morsy & Caskey 1999).

Other less inflammatory and immunogenic vectors are the AAV vectors. AAV so far has been known to make the least immunogenic response among all vectors. However, B-cell and T-cell responses can still occur towards an expressed transgene product (Thomas et al., 2000; Vandamme et al., 2017).

Specificity of Transgene Delivery/Tropism

Viral vectors have the ability to be taken up by many different cell types within numerous organs. Even if a viral vector is delivered locally, it can lead to leakage and circulation to other tissues and organs (Lewandoski 2001; Somia & Verma 2000). Systemically delivering the vector can create a large inflammatory response; similar to what was seen with Mr. Gelsinger (Thomas et al., 2003). The tropism of the different viruses can be used to help with the treatment of particular organs, while avoiding the delivery to other cell types or organs in the body (Lewandoski 2001; Somia & Verma 2000; Thomas et al., 2003).

Insertional mutagenesis

The integration of viral vector genomes into off target organs presents an obstacle for the safe delivery of gene therapeutics (Wirth et al., 2013). There are risks associated with the vectors integrating into gene regulatory areas and transcriptionally active areas, potentially causing detrimental issues with altering tumour suppressor or proto-oncogene functions and increasing oncogenesis (Wirth et al., 2013).

2.2.2 Systemic vs. Local Delivery of Gene Therapy

There are numerous methods for delivering the gene of interest into a small or large animal model. Some of the methods available are more invasive than others, especially when the disorder in question is a disease of the CNS. A systemic delivery process, such as intravenous injections, allows for a non-invasive or minimally invasive route of administration, where the AAV serotype is able to navigate from the periphery to the spinal cord (Hardcastle et al., 2018). Intramuscular, intravenous (IV) and intrathecal routes work by this delivery system (Hardcastle et al., 2018). Local delivery of AAV serotypes is an invasive surgical approach directly targeting an exact area of the spinal cord and this method is also known as intra-parenchymal delivery (Hardcastle et al., 2018).

AAV vectors can be transported from peripheral injection sites to neuronal cell bodies. This can be done through a cellular axonal transport system (Hardcastle et al., 2018). A recent study done by Benkhelifa-Ziyaat showed the retrograde axonal transport of AAV9 after delivery of a single unilateral injection of scAAV9 into the gastrocnemius muscle of a mouse model. GFP expression was found in the lumbar, thoracic, and cervical areas with transduction throughout the spinal cord (Benkhelifa-Ziyyat et al., 2013).

AAV9 vectors have the ability to cross the blood-brain-barrier (BBB) after IV administration to deliver therapeutic genes to the brain and spinal cord. Foust et al. 2009, and Duque et al. 2009; were the first to show that after IV treatment, scAAV9 crossed the BBB and was able to efficiently transduce the whole spinal cord.

Intrathecal delivery is an enticing alternative to intravenous administration. The viral vector is directly delivered into the cerebrospinal fluid (CSF) through a puncture between lumbar vertebrae. This local delivery allows for diffusion and infiltration into the spinal cord parenchyma (Hardcastle et al., 2018). Cisternal injections are also able to deliver the viral vector right into the CSF and can be just as efficient in its transducing abilities into the spinal cord (Hardcastle et al., 2018).

Intra-parenchymal injections are another form of invasive viral vector delivery into the spinal cord requiring major surgery (Hardcastle et al., 2018). This therapy is restricted to a focal area and the local injection of the viral vector needs to occur at a much lower volume than what is required for systemic delivery (Hardcastle et al., 2018).

2.2.3 Timing of treatment

Studies have been able to show how the timing of when the therapeutic vector is administered to the animal model has an effect on the likelihood that the disease will progress to its fulminant nature (Walia et al., 2015). Another study done by Osmon et al., 2016 was also able to show that neonatally injected Sandhoff mice showed correction of the Sandhoff phenotype. A study done by Cachon-Gonzalez in 2006 and 2014, using the TSD mouse model was also able to show increased survival of TSD mice that were given the therapeutic gene either before disease onset or during the early manifestation of the disease process.

After reviewing and researching the literature to date with respect to G_{M2} Gangliosidoses, current animal models, the history of gene therapy, viral vectors and the delivery and timing of treatment we proposed our current study model found in the next chapter.

Chapter 3

Current Study

Intravenous Neonatal and Adult Injection of ssAAV9/*GM2A* shows a Decrease in G_{M2} Ganglioside Storage in an AB- G_{M2} mouse model

3.1 Current Study

This proof of concept study assessed the effects of administering an ssAAV9/*GM2A* injection systemically into an AB- G_{M2} mouse model. We hypothesized that an ssAAV9/*GM2A* treatment will be able to reduce G_{M2} ganglioside storage in brains of AB- G_{M2} mice at both ages of administration. Neonatal (1-day old) and adult (6-week old) mice were injected intravenously via the superficial temporal vein and tail vein, respectively, with the viral vector containing the *GM2A* gene coding for the deficient protein. A comparable dose (as compared to doses currently used in clinical trials) was administered.

Our primary outcome measure was to see a reduction in G_{M2} ganglioside storage, biochemically, within the treated mouse mid-sections in both the 20-week and 60-week cohorts. Our secondary outcome measure was to see changes in the treated mouse phenotype in both the 20-week and 60-week cohorts through behavioural testing.

3.2 Methods

3.2.1 Plasmid construct

Artificial plasmids are used as vectors in molecular cloning in order to promote replication of recombinant DNA sequences in host organisms. For the purposes of our study the plasmid used was composed of human *GM2A*, a CAG promoter, and WPRE post-transcriptional regulatory element (Figure 3). It is a total of 2795bp. A CAG and chicken β-actin promoter were used to facilitate high levels of gene expression. A WPRE post-transcriptional regulatory element was used to increase expression of the genes delivered by the viral vector. Gene synthesis was done by Biobasic, a Toronto based research laboratory. The viral vector was constructed by a core vector facility at the University of North Carolina.

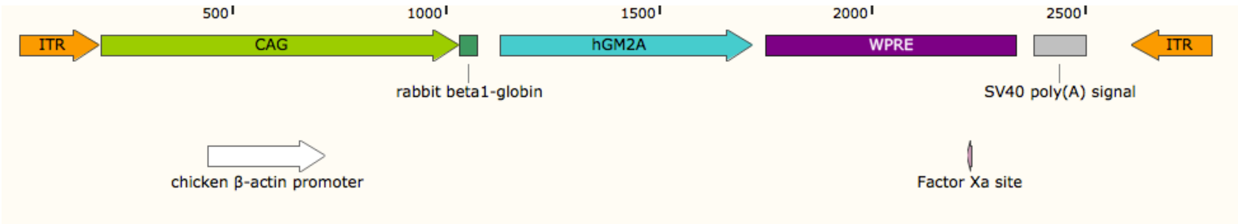

Figure 3. Human *GM2A* plasmid construct

3.2.2 Western Blot

Fibroblast cells from a donor AB- G_{M2} patient as well as AB- G_{M2} treated mouse liver tissue transfected with lipofectamine 2000 and un-transfected fibroblast cells were used. Samples were created by making a 2:1 ratio of sample to reducing buffer (B7703S – New England Buffer (NEB) 3x Reducing Blue Loading Buffer). These samples were heated to 95°C for 5 minutes, and were spun in the microcentrifuge at maximum speed (14, 000RPM or max RCF 16,000XG) for 30 seconds. Samples were quantified using the ThermoFisher Pierce ™ Bicinchoninic acid (BCA) Protein Assay Kit. 12% sodium dodecyl sulphate polyacrylamide (SDS-PAGE) gel electrophoresis was used to resolve 25µg of protein/well. Protein ladder was loaded (Precision Plus Protein ™ Kaleidoscope ™ Standards [161 - 0375] by Bio-Rad). Resolved protein samples were transferred onto a polyvinylidene fluoride (PVDF) membrane. The membrane was blocked with 5% milk and tris-buffered saline (TBS) for 2 hours at room temperature. The membrane was then incubated with primary anti-AB- G_{M2} antibody overnight at 4°C at a concentration of 1:300 in 0.5% milk and TBS; and then washed 3 times with 0.1% TBS. Next the membrane was incubated with secondary goat anti-mouse antibody (A5278 – Sigma anti-mouse, IgG –

SLBB9430 [provided by the Funk lab, Queen's University]) overnight at 4°C at a concentration of 1:10000 in 1% milk and TBS. The next day the membrane was once again washed 3 times with 0.1% TBS; and then incubated with chemiluminescent reagent (Millipore) for 3 minutes. Exposure for 20 minutes on X-ray film was done to obtain the GM2AP image. In order to get the expression for β-actin, the same membrane was washed 3 times with 0.1% tris-buffered saline-tween (TBS-T) and then blocked with 5% milk in TBS for 2 hours at room temperature. Incubation then occurred with the second primary β-actin monoclonal antibody (A5441 – Sigma anti-mouse, Lot: 064M4789 [provided by the Funk lab]) overnight at 4°C at a concentration of 1:10000 in 1% milk and 0.05% TBS-T. Once again this membrane was triple washed with 0.1% TBS-T and incubated with secondary goat anti-mouse antibody (A5278 – Sigma anti-mouse, IgG – SLBB9430 [provided by The Funk Lab, Queen's University]) overnight at 4°C at a concentration of 1:10000 in 1% milk and 0.05% TBS-T. Another triple wash with 0.1% TBS-T occurred and the membrane was exposed to an X-ray film for 5 seconds to obtain the β-actin image.

3.2.3 Experimental Animals

These studies were performed in mice homozygous for the GM2Atm1Rlp targeted mutation, which were purchased from The Jackson Laboratory. Heterozygous breeding was done to establish a colony at Queen's University. Genotyping was done on the mice colonies, using PCR amplification, to determine which mice were knock-out (KO) and heterozygous. DNA used for genotyping was extracted from mouse ear punches. Experimental mice were established by breeding knock-out (KO) mutant mice to each other. There was no method of randomization used when delivering virus, vehicle, or GFP to the experimental animals because there was no effective method of distinguishing one pup from the next in a cage at 1 day of age. The Queen's

University Animal Care Committee approved all of the procedures and protocols that the experimental mice underwent.

3.2.4 Injections

A cohort of 1-day old pups received viral vector in a dose of $1x10^{14}$ vector genomes (vg) per kilogram (kg) of mouse intravenously, total volume of 50µL, via the superficial temporal vein. Two subsequent cohorts of 1-day old pups received equal concentrations and volumes of either green fluorescent protein (GFP) treatment or 1x phosphate buffered saline (PBS). During the injection process, the mothers were removed from their cages with the pups and kept in a separate cage. Once the injections were completed, the mothers were placed back into their cages with the injected pups. Injected pups were closely monitored over a span of one week, in order to maximize survival rates of the injected mice. Viral vector in a dose of $1x10^{14}$ vg/kg of mouse was also injected intravenously (50µL) into a cohort of 6-week-old adult mice via tail vein. Please refer to Table 3 for treatment cohorts for both 20- and 60-week time points.

Cohort Number	Genotype	Treatment	Age of Delivery	Dose (vg/kg)	Number in Cohort Endpoint (Age)	
					20 wk	60wk
1	Heterozygous (+/-)	None		-	6	6
2	GM2A (-/-)	ssAAV9/*GM2A*	1-2 days	$1x10^{14}$	6	6
3	GM2A (-/-)	ssAAV9/GFP	1-2 days	$1x10^{14}$	6	6
4	GM2A (-/-)	Vehicle	1-2 days	-	6	6
5	GM2A (-/-)	ssAAV9/*GM2A*	6 weeks	$1x10^{14}$	6	6
				TOTAL	30	30

Table 3. Treatment cohorts for both 20- and 60-week time points

3.2.5 Behavioural Testing

The experimental mice underwent a battery of behavioural tests, including the Rotarod Test (RR), the Open Field Test (OFT), and the Weight Test. The testing began at 8 weeks of age and continued monthly, until the predetermined endpoint of either 20-weeks or 60-weeks for the short and long-term cohorts, respectively. Motor coordination of the mice was assessed using a RR apparatus (IITC Life Sciences) ([JoVE] Osmon et al., 2018). In this test the mouse was put on a rotating cylinder, which is suspended over a balancing floor/beam. The mouse would try to stay on the rotating cylinder and would try to avoid falling onto the balancing floor/beam. The mouse's latency to fall, distance travelled and end rotations per minute (RPM) were measured while on the apparatus. An accelerated protocol was used and the rod increased in speed from 4rpm to 40rpm over a 5-minute time period. Three trials were given to each mouse and the trial in which the mouse remained on the rotating cylinder for the longest length of time was kept for data analysis.

The next test in the battery of behavioural testing was the OFT, which measures the general locomotor activity of the mice. The open field apparatus was a white plywood floor covered by 4 white plywood walls (to create a box without a lid); 3 feet in height on all 4 sides. A video camera with associated software (SmartWare) was able to assess the mouse's activity. Parameters such as the time resting, time moving, distance travelled and mean speed were recorded. The mouse was placed in the center of the OFT apparatus and the timer was started simultaneously. Each mouse was assessed in the OFT for a total of 5 minutes.

Lastly, to measure the mice's strength in their limbs a muscle strength test was conducted. Large paper clips equal in weight to the previous clip, were added to a wire mesh one-by-one. Each jumbo paper clip weighed 7.5grams each. Initially, one paper clip would be added to the wire mesh and the mouse would hold onto the wire mesh (steel wool pad) with its forepaws and would be timed for a maximum of 3.0 seconds. The experimenter would be holding on to the mouse tail during this time. If the mouse held on for the full 3.0 seconds, then a second paper clip would be added to the wire mesh and the mouse would be timed until they let go of the wire mesh. Mice would have at least a 10 second break between weight additions onto the wire mesh. A maximum of 5 paper clips would be added to the wire mesh. In order to get a total strength measurement for each mouse, the time (in seconds) the mouse held on to the wire mesh would be multiplied by the number of weights on the wire mesh up to a maximum of 15.

Behavioural testing for the 20-week neonatal and adult cohorts were done during the light-cycle on a monthly basis; and this testing was done by the primary author (M.V.). The 60-week neonatal and adult cohorts had behavioural testing done during the light-cycle on a monthly basis as well; however, the testing after 30-weeks was done by the secondary author (N.D.). Neither of the individuals performing the behavioural testing were blinded to the different mice cohorts.

3.2.6 Tissue and Serum Collection

Monthly saphenous vein blood collections were done on the experimental mice starting at 8 weeks of age, usually occurring sequentially after behavioural testing. The final blood collection was done at the mouse's euthanization time point via cardiac puncture. Once the blood had been collected, it was then separated by centrifugation at 3500 rotations per minute (RPM) for a total of 10 minutes and the serum was stored at -20C.

Tissue samples were collected at the short-term (20-weeks) and long-term (60-weeks) predetermined endpoints for all neonatal and adult experimental KO, GFP, vehicle and heterozygous mice. Mice were euthanized via CO_2 asphyxiation, and a pinch-test was performed on each mouse to ensure that they were fully euthanized before performing a cardiac puncture, followed by perfusing the mouse systemically with 1x PBS via the left heart ventricle. A mid-section from the brain was taken and placed in a paraformaldehyde solution (as shown in figure 4). After 24 hours of submersion in paraformaldehyde, the mid-section was placed in a histology cassette and submerged in 100% ethanol for at least 24 hours before being embedded in paraffin wax. Cervical and lumbar spinal cord tissue was also excised for histology. Other organ tissue samples that were taken include: heart, lungs, kidneys, gonads, arm muscle, liver and spleen. These tissue samples were then frozen at -20ºC.

3.2.7 G_{M2} Ganglioside Storage Assay

The quantification of the G_{M2} ganglioside storage assay was carried out over a 3-day period (Folch et al., 1951; Tropak et al., 2010; Wherrett & Cumings, 1963). On the first day of the protocol, PBS was added to the frozen mid-sections and sonicated for three 10-second pulses at an amplitude of 20%. These samples were then spun down at maximum speed (15,500RPM or max RCF 21,200xG) in a centrifuge set to 4ºC for a total of 20 minutes. 300µL of the supernatant was then mixed with the pellet along with methanol and chloroform and incubated overnight. During the second day, the samples were centrifuged, diluted with varying volumes of methanol/chloroform/PBS and water. Gangliosides were isolated using C-12 columns, and then the solvents were evaporated with nitrogen gas. On day-3 the thin layer chromatography (TLC) tank was first prepared by adding chloroform:methanol:CaCl2 in a ratio of 55:45:10 at the bottom of the tank. The TLC plate was then used to separate the experimental ganglioside samples from the previous day. A ganglioside cocktail control was also run with the ganglioside samples. Orcinol staining was used in order to see the various bands of gangliosides and the TLC plate was then dried in an oven set to 120C for 8-10 minutes. ImageJ software was used to compare the intensity of the bands seen for G_{M2} compared to GD1A, this allowed for a final graph to be created to assess whether there was a decrease in G_{M2} ganglioside storage.

3.2.8 Copy Number Analysis qRT-PCR

The qPCR method was used to determine the copy numbers of the hGM2AP vector and mouse genomic DNA. A gSYNC™ DNA Extraction Kit (cat. no. GS100; Geneaid) was used to extract the total DNA from each organ. PowerUp SYBR Green Master Mix (cat. no. A75242; Thermo Fisher) on the Applied Biosystems® 7500 Real-Time PCR Systems was used by following the manufacturer's instructions, for each of the reactions. Plasmid DNA was used as the standard for virus quantitation. Purified and quantified mouse genomic DNA was used as a standard for mouse genomic DNA quantitation. Primers for virus pAAv.CAG.hGM2A.WPRE were as follows: (forward) 5′- TATGGGCTTCCTTGCCACTG -3′, (reverse) 5′-

CTCAGGACGCTCTCTATGCG -3′. Mouse LaminB2 primers for quantitation of mouse genomic DNA were as follows: (forward) 5′- GGACCCAAGGACTACCTCAAGGG -3′, (reverse) 5′- AGGGCACCTCCATCTCGGAAAC -3′.

3.2.9 Histology

Fresh organ tissues were fixed in 4% paraformaldehyde (PFA) for 24 hours, then immersed in 100% ethanol (EtOH) for 24 hours before sending for processing and embedding in paraffin. Paraffin embedded samples were then sectioned to a thickness of 4-6μM using a microtome, dried and baked at 60°C for overnight. Samples were then de-paraffinized, rehydrated and placed into an antigen retrieval solution. There was blocking of endogenous peroxidase activity as well as blocking of non-specific binding. The sections were placed in primary anti-AB- G_{M2} antibody KM966 (donated by The Funk Lab, Queen's University) at 1:1000 and then detected using biotinylated human secondary antibody at 1:1000. DAB (3,3'diaminobenzidine) staining was done and after this application the slides were dehydrated initially in 70% EtOH, then 85% EtOH, and lastly 100% EtOH.

Histology Brain Sections

In order to obtain the brain section for histology staining we initially divided the mouse brain into 3 gross divisions of the rostral section of brain, mid-section and caudal section of brain by using a mouse brain mold. Please refer to Figure 4. We kept the mouse brain intact in a brain mold and then used a blade to cut out a 2mm section from the center of the mid-section brain area and then transferred this section into an Eppendorf tube filled with 4% PFA. Cutting a clean section of the mouse brain served to be a difficult task; and we chose this specific 2mm area of the brain because it provided us with the largest surface area to analyze. When deciding what areas of the histology sections to include in the results section we initially looked at the entire brain section that we had obtained. Both hemispheres showed equal staining and therefore we chose one hemisphere to obtain our histology images; which included the hypothalamus, thalamus and hippocampus, for each of the cohorts. Please refer to Table 4 for a flow diagram that includes a summarized version of the full study. We were unable to successfully section usable sections of the mouse cerebellum for histological staining.

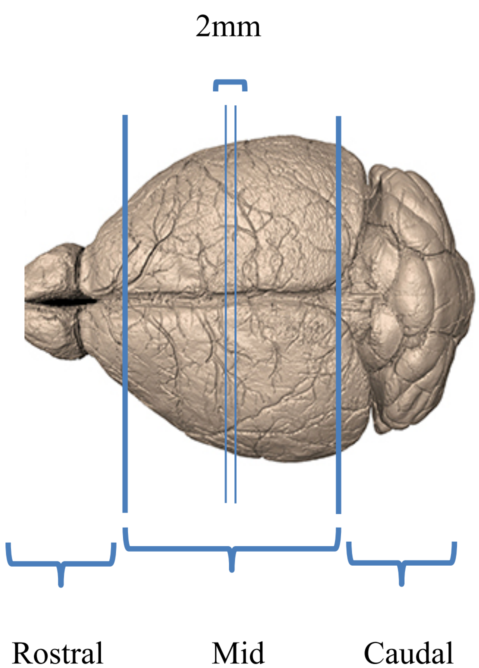

Figure 4. Schematic diagram of mouse brain. Gross divisions of mouse brain shown as rostral section, mid-section and caudal sections. (Mouse brain image adapted from Xiong et al., 2017).

3.2.10 Statistics

Statistical analysis was done using GraphPad Prism 8 for Mac. The G_{M2} ganglioside storage assay analysis for 20 week and 60-week endpoints were done using one-way ANOVAs with Tukey's multiple comparisons. The behavioural testing from 8 weeks until 20-weeks for the short-term cohort as well as the behavioural testing from 8 weeks until 60-weeks for the long-term cohort was analyzed using 2-way repeated-measure analysis of variance (ANOVA) (Mixed effects model) with Dunnett's multiple comparisons. All of the behavioural testing data did not show statistically significant data for the 2-way repeated-measure ANOVA's; however we still opted to complete multiple comparisons on this data.

Table 4. Flow diagram of study. 20-week and 60-week time points and the behavioural testing and biochemical testing done for each cohort; including polymerase chain reaction (PCR), biochemistry (BC) and histology (Hist).

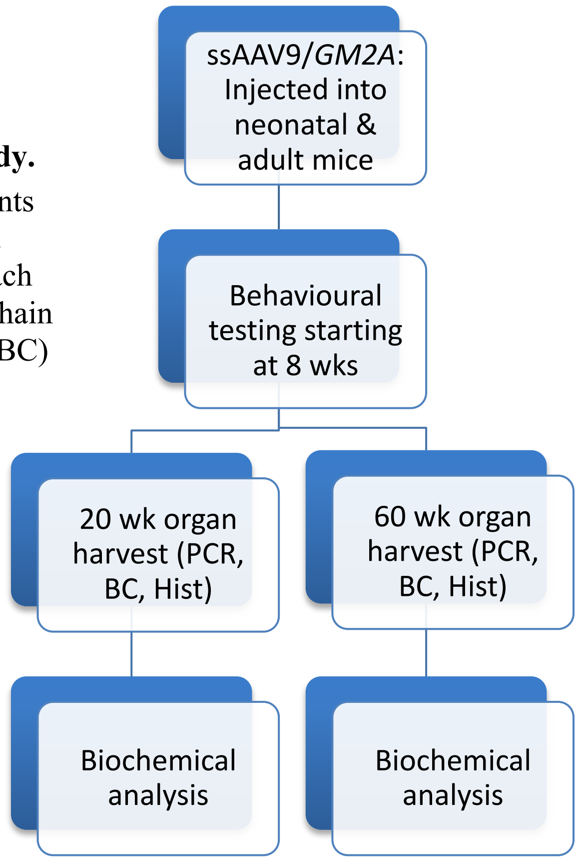

3.3 Results

3.3.1 Western Blot Analysis

Western blot analysis was done using an AB- G_{M2} patient fibroblast showing no GM2AP expression. The western blot was able to show GM2AP expression at 24- and 48hr post-transfection. A treated mouse liver sample was included and showed GM2AP expression. The house-keeping β-actin protein was seen in all samples. Please refer to Figure 5.

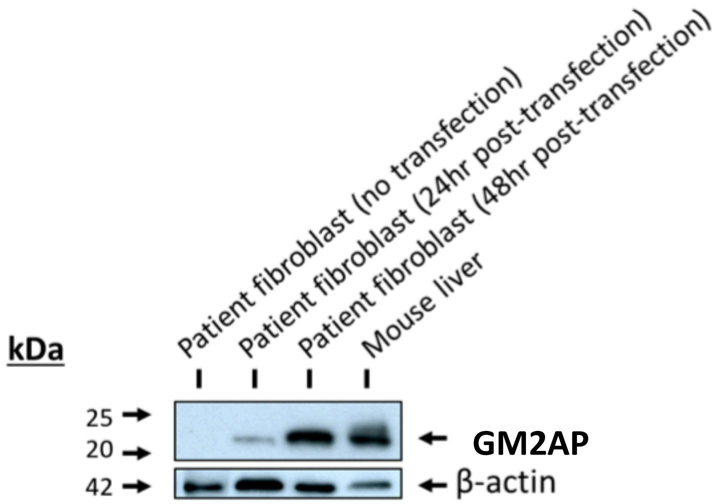

Figure 5. Western Blot Analysis

For Confirmatory GM2AP expression. Patient fibroblast is GM2AP -/- (KO, mutant). Mouse liver is GM2AP -/- (adult virus treated). β-actin protein is a house-keeping protein seen in all samples.

GM2AP is a 21kDa protein.

Final western blot presented here has been completed by Chris Richmond MSc. Candidate from The Funk Lab.

3.3.2 Biochemical Ganglioside Storage Analysis

The short-term and long-term cohorts both showed a reduction in the amount of G_{M2} ganglioside storage in the treated mice compared to the vehicle treated mice (Figure 9). In the short-term cohort there was a significant effect of treatment in the mid-section samples of the 1-day old neonatal treated mice and the 6-week adult treated mice in comparison to the vehicle KO mice ($p < 0.05$) (Figure 9A). In the short-term cohort we were able to deduce a 55% reduction in G_{M2} ganglioside storage in the neonatal treated mice compared to the vehicle treated mice; and a 73% reduction in G_{M2} ganglioside storage in the 6-week treated mice compared to the vehicle treated mice (Figure 9A).

In the long-term cohort there was no significant effect of treatment in the mid-section samples of the 1-day neonatal treated mice and 6-week adult treated mice (Figure 9B). In the long-term cohort we were able to deduce a 12% decrease in G_{M2} ganglioside storage in the neonatal treated mice compared to the vehicle treated mice; and a 29% decrease in G_{M2} ganglioside storage in the 6-week treated mice compared to the vehicle treated mice (Figure 9B).

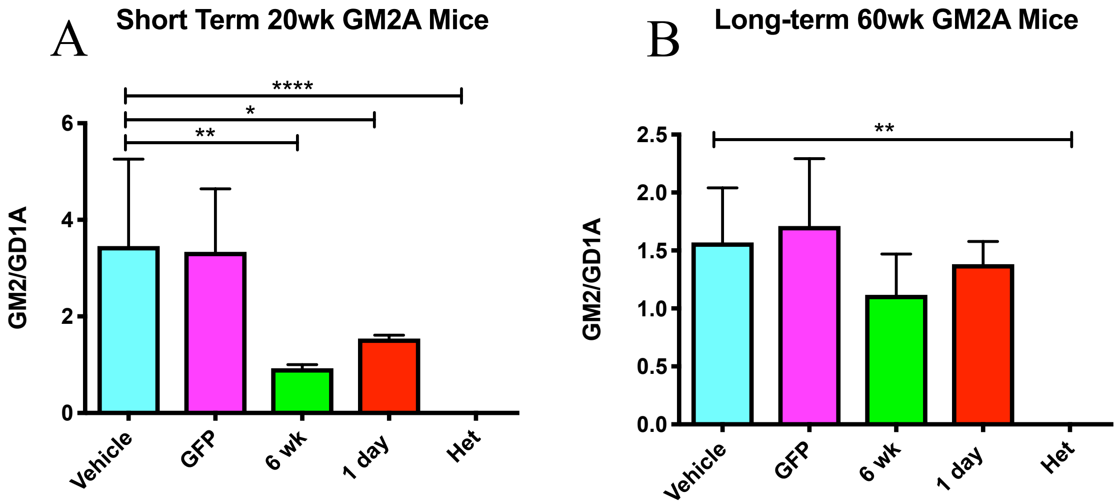

Figure 9. G_{M2} Ganglioside Storage Analysis of Brain Mid-section Samples

Overall the neonatal treated and adult treated cohorts stored less G_{M2} gangliosides in comparison to the knock out (vehicle) cohort; in both the short-term and long-term cohorts. (A) In the 20-week cohort the neonatal treated group (n=5) and the adult treated group (n=6) differed significantly from the vehicle treated group (n=6) ($p<0.05$) and the heterozygous group (n=6) ($p<0.0001$). (B) In the 60-week cohort the heterozygous group (n=5) differed significantly from the vehicle group (n=4) ($p<0.05$), the 6-week adult treated group (n=5) ($p<0.05$), the neonatal virus treated group (n=4) ($p<0.001$), and the GFP treated group (n=4) ($p<0.05$).

Behavioural Outcomes

3.3.3 Short Term Findings

The neonatal and adult treated cohorts were not able to significantly outperform their vehicle counterparts in the majority of the behavioural testing measures. The general locomotor activity of the mice was tested using the Open Field Test (OFT) for the short-term 20-week cohort. The distance travelled, mean speed, and resting time in the apparatus were measured. Motor coordination was tested using the RotaRod (RR) for the short-term 20-week cohort. The end rotations per minute (End-RPM), latency to fall and distance travelled were measured. The muscular strength test measured the strength of the various murine cohorts at the short-term 20-week time points.

In the OFT- distance travelled from 8-20 weeks there was a significant time effect $F(3, 104) = 4.314$; $p = 0.0066$ (Figure 6A). Overall, the groups differed significantly over time $F(4, 104) = 3.090$; $p = 0.0190$. However, there was no time by treatment interaction (Figure 6A).

In the OFT- mean speed from 8-20 weeks there was no time effect; groups did not differ significantly over time and there was no time by treatment interaction (Figure 6B).

In the OFT-resting time from 8-20 weeks there was a significant time effect $F(3, 78) = 9.641$; $p<0.0001$ (Figure 6C). Overall, the groups differed significantly over time $F(4, 26) = 2.775$; $p = 0.0481$. There was a significant time by treatment interaction $F(12, 78) = 2.548$; $p = 0.0068$. (Figure 6C).

In the RR-End RPM from 8-20 weeks there was a significant time effect $F(3, 78) = 4.723$; $p = 0.0044$ (Figure 6D). Overall, the groups did not differ significantly over time. However, there was a time by treatment interaction $F(12, 78) = 2.288$; $p = 0.0150$ (Figure 6D).

In the RR-latency to fall from 8-20weeks there was a significant time effect $F(3, 78) = 6.210$; $p = 0.0008$ (Figure 6E). The groups did not differ significantly over time. There was a time by treatment interaction $F(12, 78) = 3.439$; $p = 0.0004$ (Figure 6E).

In the RR-distance travelled from 8-20weeks there was no significant time effect and the groups did not differ significantly over time (Figure 6F). There was a time by treatment interaction $F(12, 78) = 2.220$; $p = 0.0183$.

A

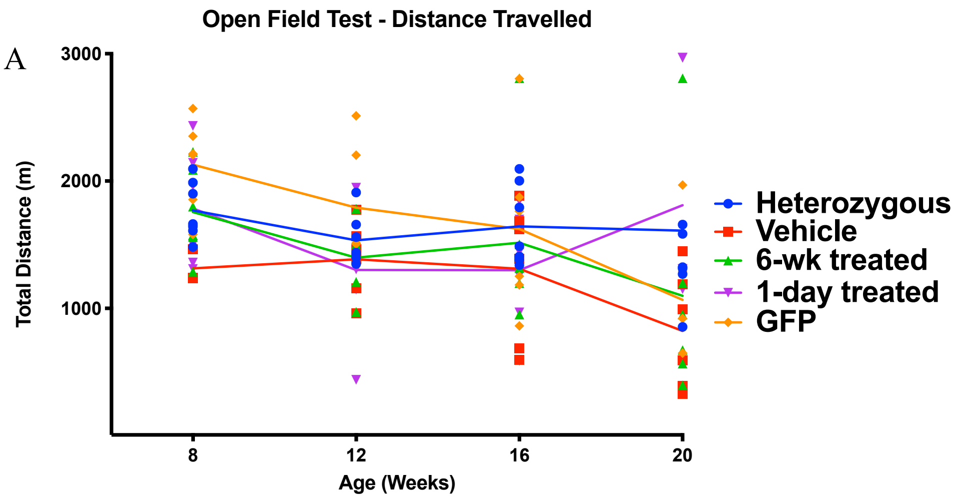
Open Field Test - Distance Travelled
3000
2000
1000
Total Distance (m)
8
12
16
20
Age (Weeks)
Heterozygous
Vehicle
6-wk treated
1-day treated
GFP

B

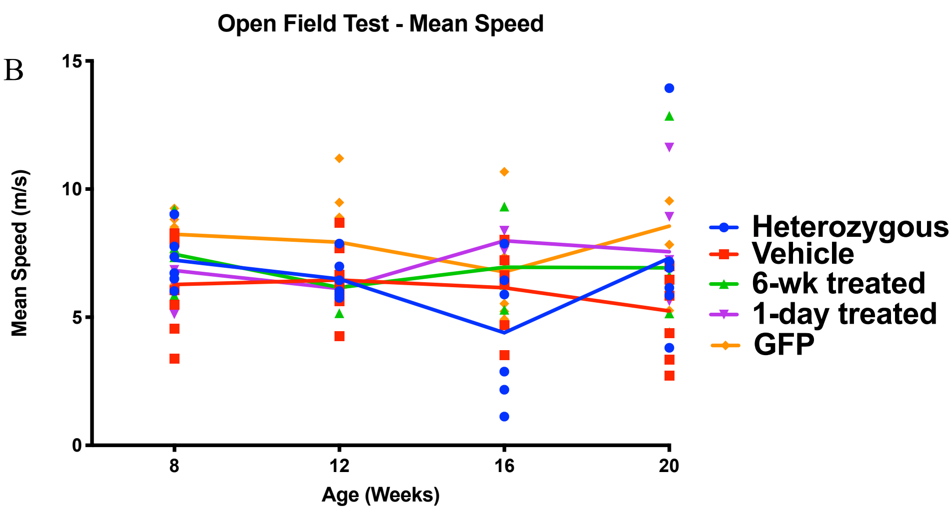
Open Field Test - Mean Speed
15
10
5
0
Mean Speed (m/s)
8
12
16
20
Age (Weeks)
Heterozygous
Vehicle
6-wk treated
1-day treated
GFP

C

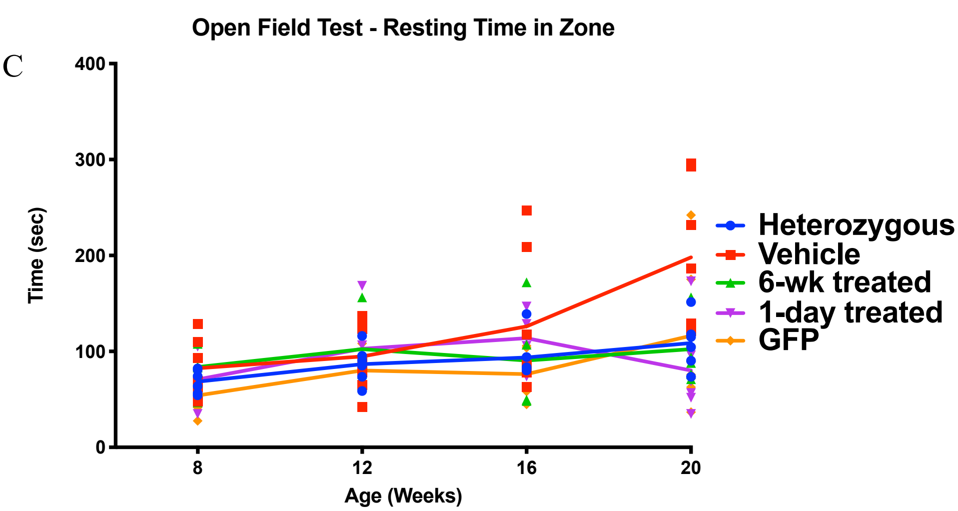
Open Field Test - Resting Time in Zone
400
300
200
100
0
Time (sec)
8
12
16
20
Age (Weeks)
Heterozygous
Vehicle
6-wk treated
1-day treated
GFP

D

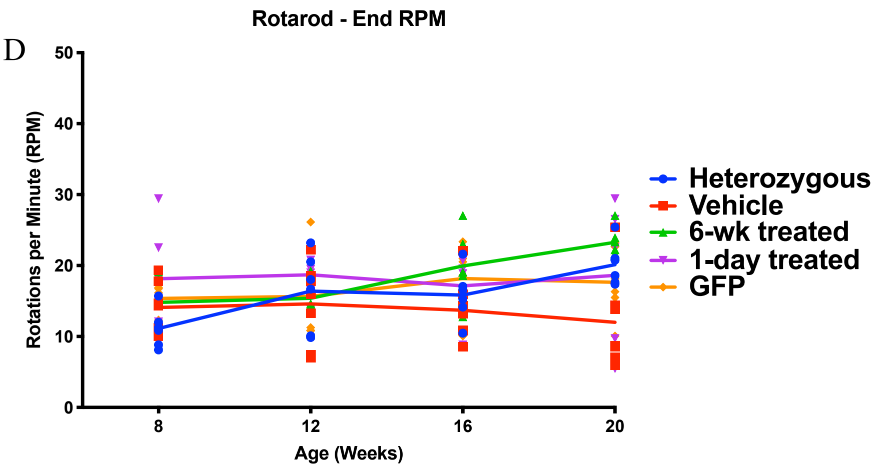
Rotarod - End RPM
Rotations per Minute (RPM)
0
10
20
30
40
50
8
12
16
20
Age (Weeks)
Heterozygous
Vehicle
6-wk treated
1-day treated
GFP

E

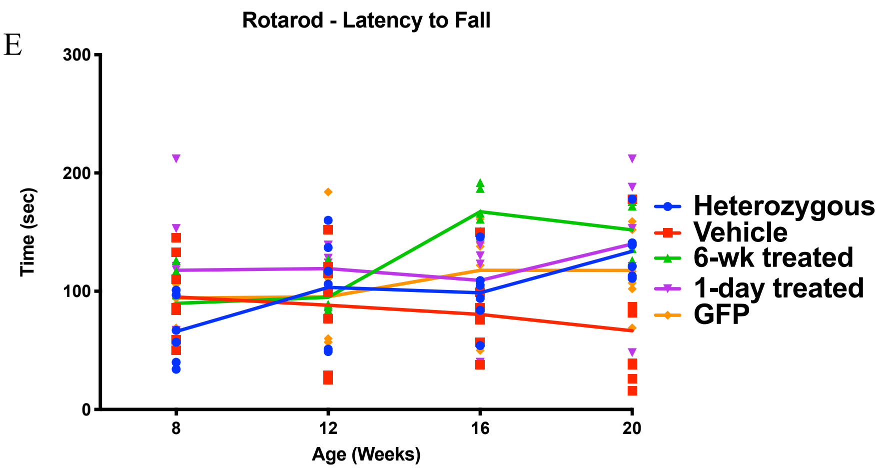
Rotarod - Latency to Fall
Time (sec)
0
100
200
300
8
12
16
20
Age (Weeks)
Heterozygous
Vehicle
6-wk treated
1-day treated
GFP

F

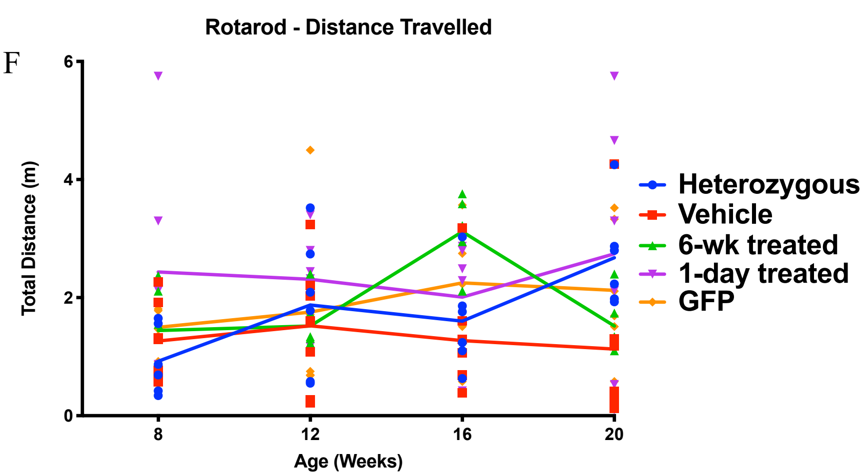
Rotarod - Distance Travelled
Total Distance (m)
0
2
4
6
8
12
16
20
Age (Weeks)
Heterozygous
Vehicle
6-wk treated
1-day treated
GFP

Figure 6. Short-term 20 week Behavioural Analysis of ssAAV9/*GM2A* treatment.

Behavioural outcomes of the heterozygous group (n=6), the untreated vehicle KO group (n=6), 6-week old adult treated group (n=6), 1-day old neonatal treated group (n=5), and the untreated GFP group (n=6) from 8 weeks to their human endpoint of 20-weeks.

The neonatal and adult treated cohorts were not able to significantly outperform their vehicle counterparts in the majority of the behavioural testing measures. Open Field Test-Distance Travelled from 8 - 20-weeks (A). Open Field Test-Mean Speed from 8 - 20-weeks (B). Open Field Test-Resting Time from 8 - 20-weeks (C). RotaRod-End RPM from 8 - 20-weeks (D). RotaRod-Latency to Fall from 8 - 20-weeks (E). RotaRod-Distance Travelled from 8 - 20-weeks (F).

3.3.4 Long Term Findings

The neonatal and adult treated cohorts were not able to significantly outperform their vehicle counterparts in the majority of the behavioural testing measures. The general locomotor activity of the mice was tested using the Open Field Test (OFT) for the short-term 60 week cohort. The distance travelled, mean speed, and resting time in the apparatus were measured. Motor coordination was tested using the RotaRod (RR) for the short-term 60 week cohort. The end rotations per minute (End-RPM), latency to fall and distance travelled were measured. The muscular strength test measured the strength of the various murine cohorts at the short-term 60 week time points.

In the OFT – distance travelled from 8 – 60 weeks there was a significant time effect $F(13, 286) = 34.36$; $p = <0.0001$ (Figure 7A). The groups did not differ significantly over time. There was a time by treatment interaction $F(52, 286) = 1.893$ (Figure 7A).

In the OFT- mean speed from 8-60 weeks there was a significant time effect $F(13, 286) = 3.090$; $p = 0.0003$ (Figure 7B). The groups did not differ significantly over time. There was a time by treatment interaction $F(52, 286) = 1.618$ (Figure 7B).

In the OFT-resting time from 8-60 weeks there was a significant time effect $F(13, 286) = 42.65$; $p < 0.0001$ and a significant difference between groups over time $F(4, 22) = 4.012$; $p = 0.0136$ (Figure 7C). There was a time by treatment interaction $F(52, 286) = 2.041$; $p = 0.0001$ (Figure 7C).

In the RR-End RPM from 8-60 weeks there was no significant time effect. There was a significant difference between the groups over time $F(4, 22) = 4.800$; $p = 0.0062$ (Figure 7D). There was no time by treatment interaction.

In the RR-latency to fall from 8-60weeks there was no significant time effect; but there was a significant difference between the groups over time $F(4, 22) = 4.845$; $p = 0.0059$ (Figure 7E). There was a time by treatment interaction $F(52, 286) = 1.526$; $p = 0.0168$ (Figure 7E).

In the RR-distance travelled from 8-60weeks there was no significant time effect, but there was a significant difference between the groups over time $F(4, 22) = 4.553$; $p = 0.0079$ (Figure 7F). There was no time by treatment interaction.

A

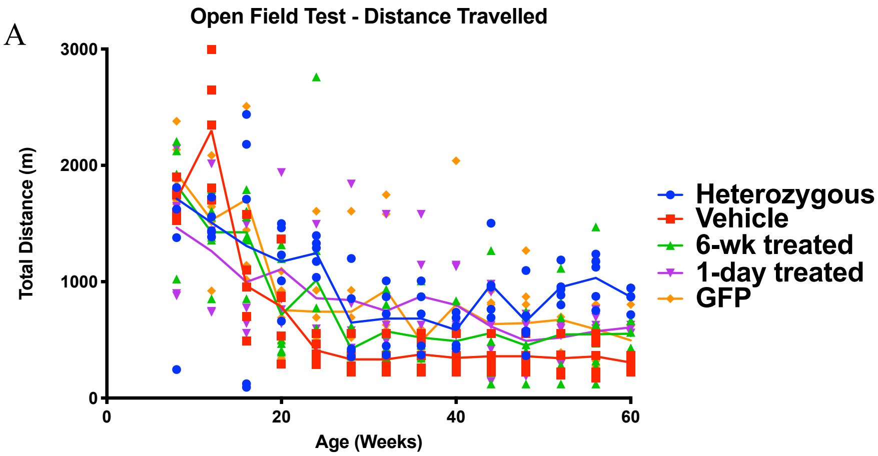
Open Field Test - Distance Travelled
Total Distance (m)
Age (Weeks)
Heterozygous
Vehicle
6-wk treated
1-day treated
GFP

B

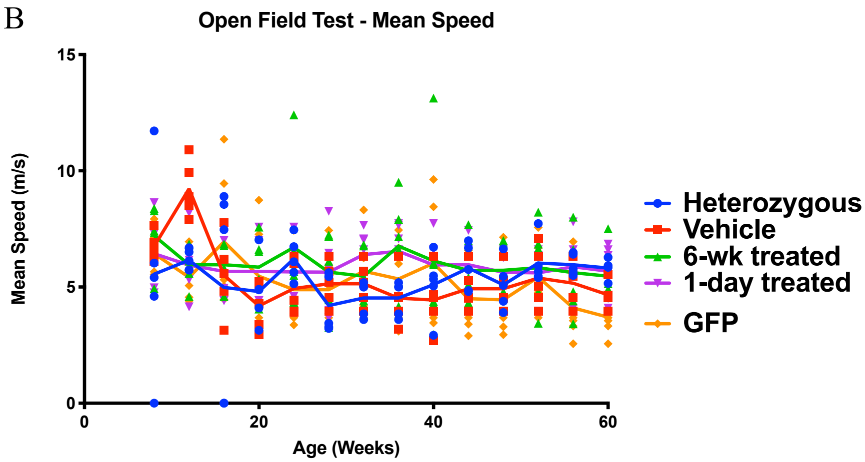
Open Field Test - Mean Speed
Mean Speed (m/s)
Age (Weeks)
Heterozygous
Vehicle
6-wk treated
1-day treated
GFP

C

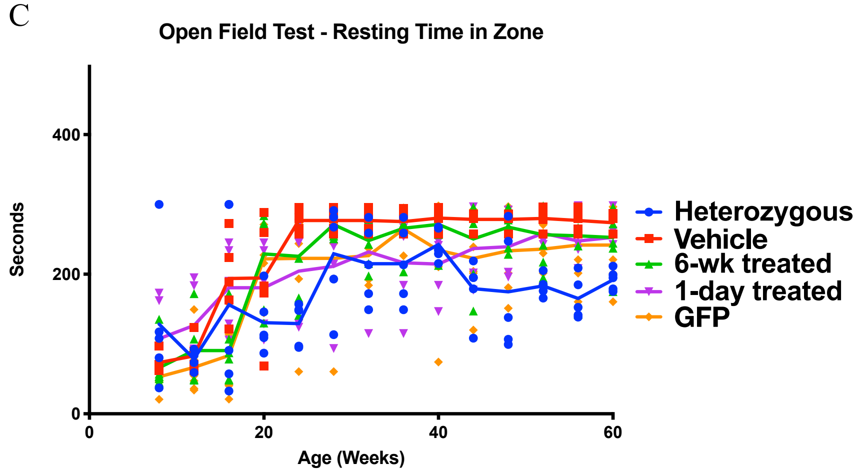
Open Field Test - Resting Time in Zone
Seconds
Age (Weeks)
Heterozygous
Vehicle
6-wk treated
1-day treated
GFP

D

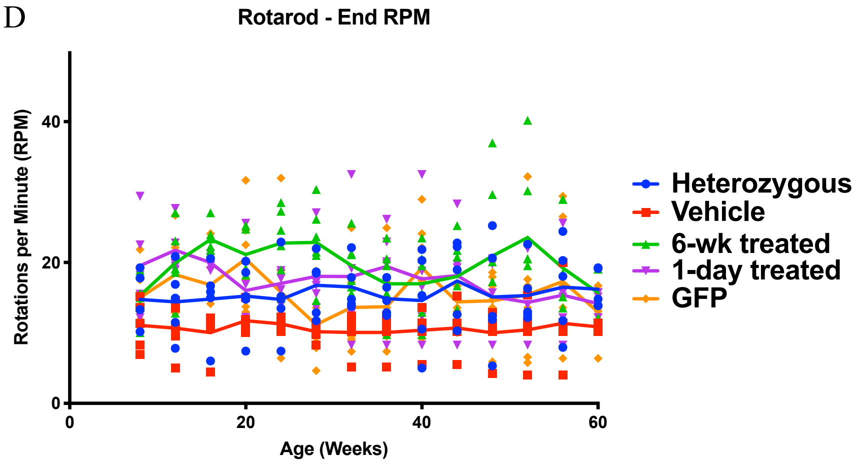
Rotarod - End RPM
Rotations per Minute (RPM)
0
20
40
0
20
40
60
Age (Weeks)
Heterozygous
Vehicle
6-wk treated
1-day treated
GFP

E

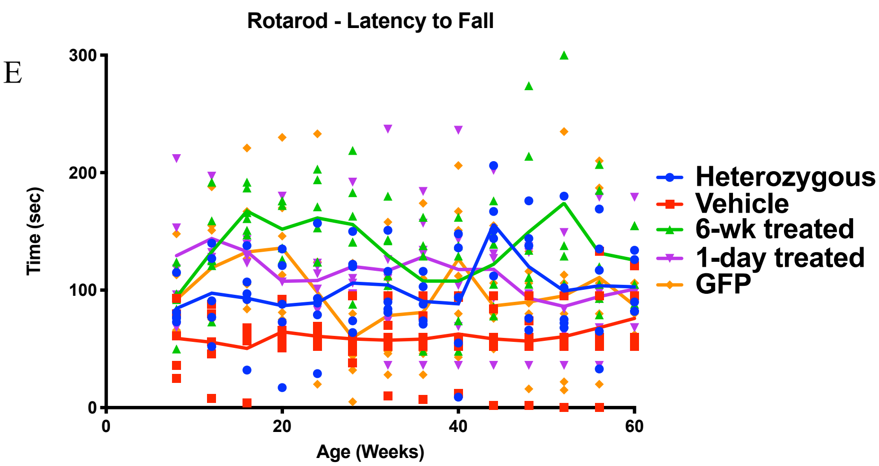
Rotarod - Latency to Fall
Time (sec)
0
100
200
300
0
20
40
60
Age (Weeks)
Heterozygous
Vehicle
6-wk treated
1-day treated
GFP

F

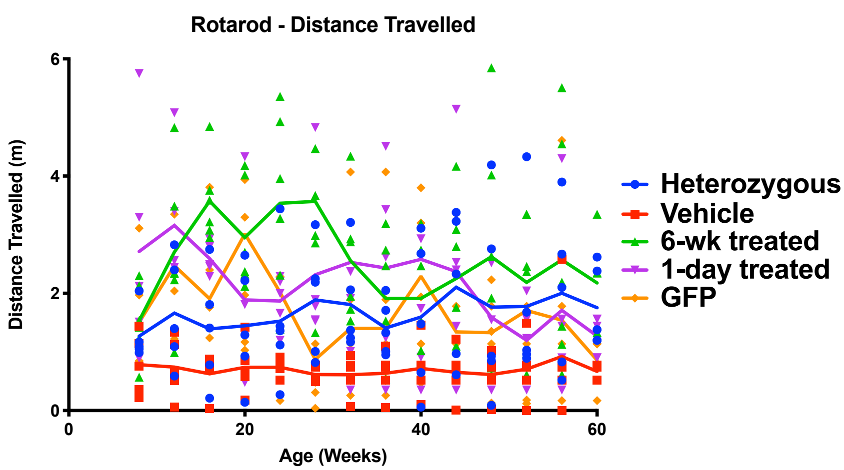
Rotarod - Distance Travelled
Distance Travelled (m)
0
2
4
6
0
20
40
60
Age (Weeks)
Heterozygous
Vehicle
6-wk treated
1-day treated
GFP

Figure 7. Long-term 60 week Behavioural Analysis of ssAAV9/*GM2A* treatment.
Behavioural outcomes of the heterozygous group (n=5), the untreated vehicle group (n=3), 6-week old adult treated group (n=5), 1-day old neonatal treated group (n=4), and the untreated GFP group (n=4) from 8 weeks to their humane endpoint of 60 weeks. The neonatal and adult treated cohorts were not able to significantly outperform their vehicle counterparts in the majority of the behavioural testing measures. Open Field Test Distance Travelled from 8 - 60 weeks (A). Open Field Test Resting Time from 8 - 60 weeks (B). Open Field Test Mean Speed from 8 - 60 weeks (C). RotaRod End RPM from 8 - 60 weeks (D). RotaRod Latency to Fall from 8 - 60 weeks (E). RotaRod Distance Travelled from 8 - 60 weeks (F). 40-60 week behavioural testing for long-term cohort completed by Natalie Deschenes PhD Candidate Walia Lab.

3.3.5 Muscular Strength Test Findings for 20- and 60-week cohorts

The neonatal and adult treated cohorts were not able to significantly outperform their vehicle counterparts in the majority of the behavioural testing measures. The general muscular strength of the mouse was tested using the Muscular Strength Test for the 8-20week, short term cohort and the 8-60week, long term cohorts.

In the 20-week cohort there was no significant time effect, but there was a significant difference between the groups over time $F(4,25) = 12.22$; $p < 0.0001$ (Figure 8A). There was a time by treatment interaction $F(12,75) = 5.257$; $p < 0.0001$.

In the 60-week cohort there was a significant time effect $F(13, 286) = 10.94$; $p < 0.0001$ (Figure 8B). There was no significant difference of groups over time. However, there was a time by treatment interaction $F(52,286) = 3.332$; $p < 0.0001$.

A

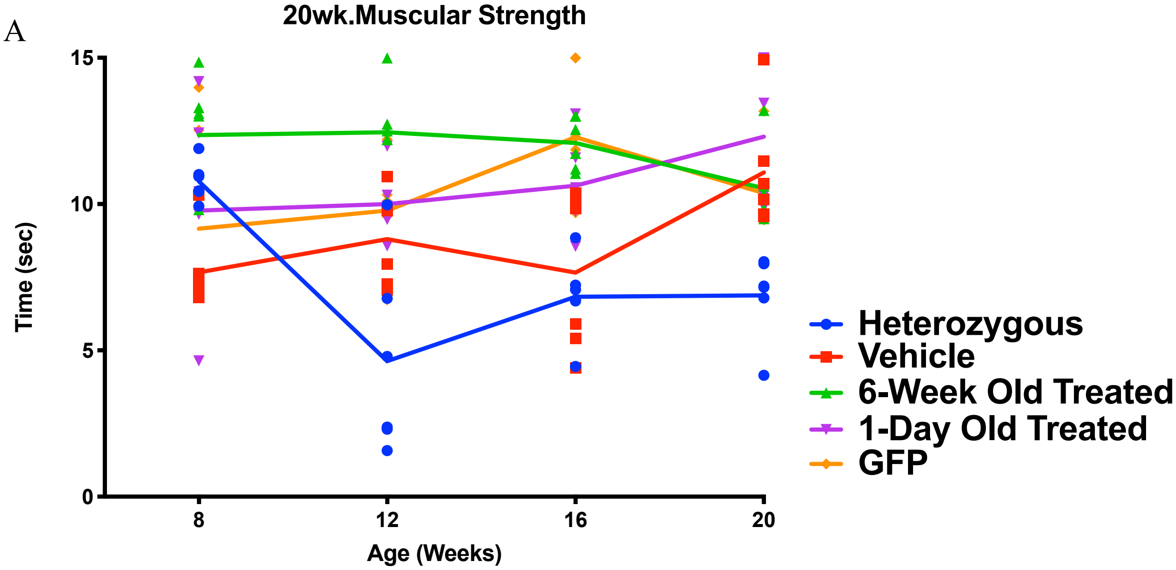
20wk.Muscular Strength
Time (sec)
Age (Weeks)
Heterozygous
Vehicle
6-Week Old Treated
1-Day Old Treated
GFP

B

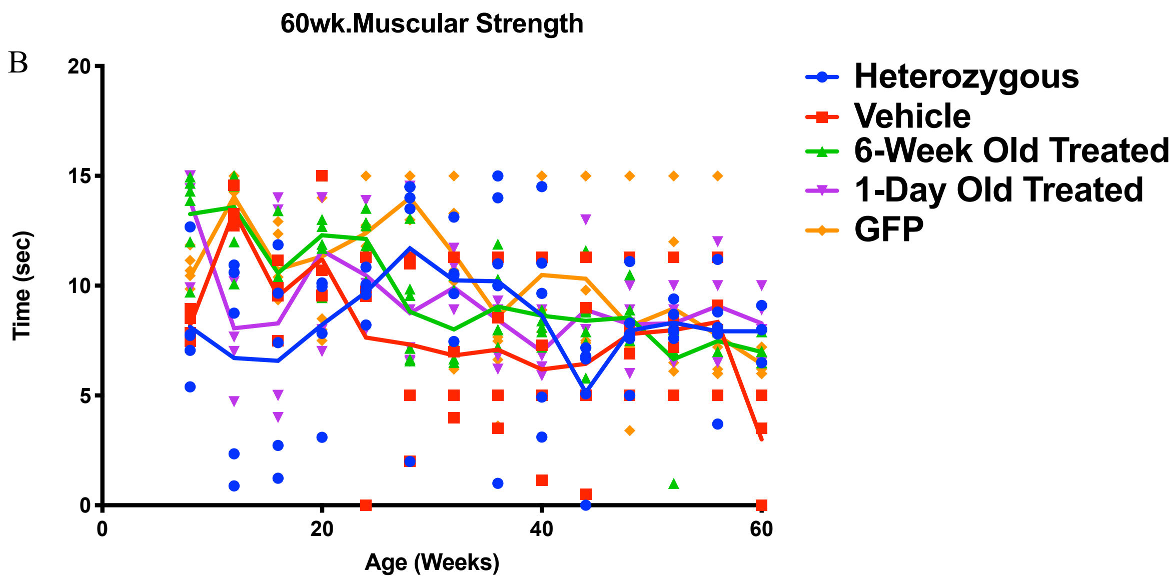
60wk.Muscular Strength
Time (sec)
Age (Weeks)
Heterozygous
Vehicle
6-Week Old Treated
1-Day Old Treated
GFP

Figure 8. 20-week and 60-week Muscular Strength Test

(A) For the 20-week cohort – Muscular strength test outcomes of the heterozygous group (n=6), the untreated vehicle KO group (n=6), 6-week old adult treated group (n=6), 1-day old neonatal treated group (n=5), and the untreated GFP group (n=6) from 8 weeks to their human endpoint of 20-weeks. (B) For 60-week cohort – Muscular strength test outcomes of the heterozygous group (n=5), the untreated vehicle group (n=3), 6-week old adult treated group (n=5), 1-day old neonatal treated group (n=4), and the untreated GFP group (n=4) from 8 weeks to their humane endpoint of 60 weeks. The neonatal and adult treated cohorts were not able to significantly outperform their vehicle counterparts in the majority of the behavioural testing measures.

3.3.6 Biodistribution of ssAAV9/*GM2A* in the brain and liver

A qT-PCR method was used to analyze the spread of the intravenously injected virus into the mice cohorts. GM2AP was expressed in all three areas of the brain regions as well as the liver in both the short- and long-term cohorts (Figure 10).

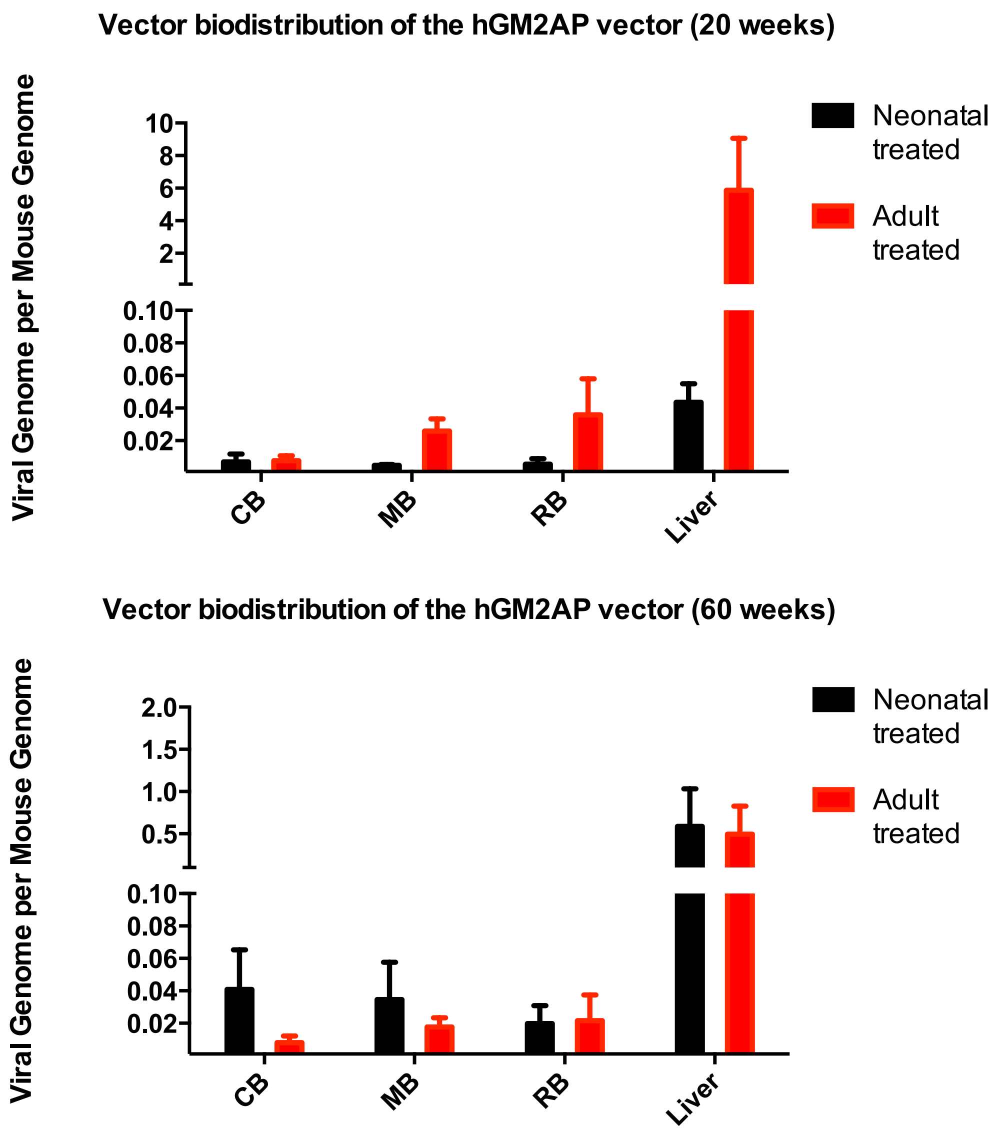

Figure 10. Biodistribution of the hGM2AP vector in the 20-week and 60-week cohorts.

Vector biodistribution of the hGM2AP vector. Viruses distributed in three parts of brain and liver in the neonatal and adult mice. hGM2AP was not detectable above 0.00 copies per mouse genome in AB- G_{M2} mice, and mice dosed with vehicle and GFP virus, and therefore is not shown on the graph. Data are presented as the copies of vector DNA per diploid mouse genome found in each assessed organ. Lamin B2 was used as a control. q-PCR method and graphs completed by Zhilin Chen, Lab Technician in Walia Lab.

3.3.7 Histological Ganglioside Storage Analysis

Paraffin embedded brain samples were sliced using a microtome and then stained with an anti-G_{M2} ganglioside antibody after which visualization was done using a secondary antibody. In comparing the vehicle cohort and ssAAV9/*GM2A* treated cohort along with the heterozygous group, there was increased G_{M2} ganglioside staining evident in the hypothalamus, thalamus and hippocampus in the vehicle KO groups and decreased amounts of G_{M2} ganglioside build up in the heterozygous and treated groups in both the 20- and 60-week cohorts (Figure 11).

A

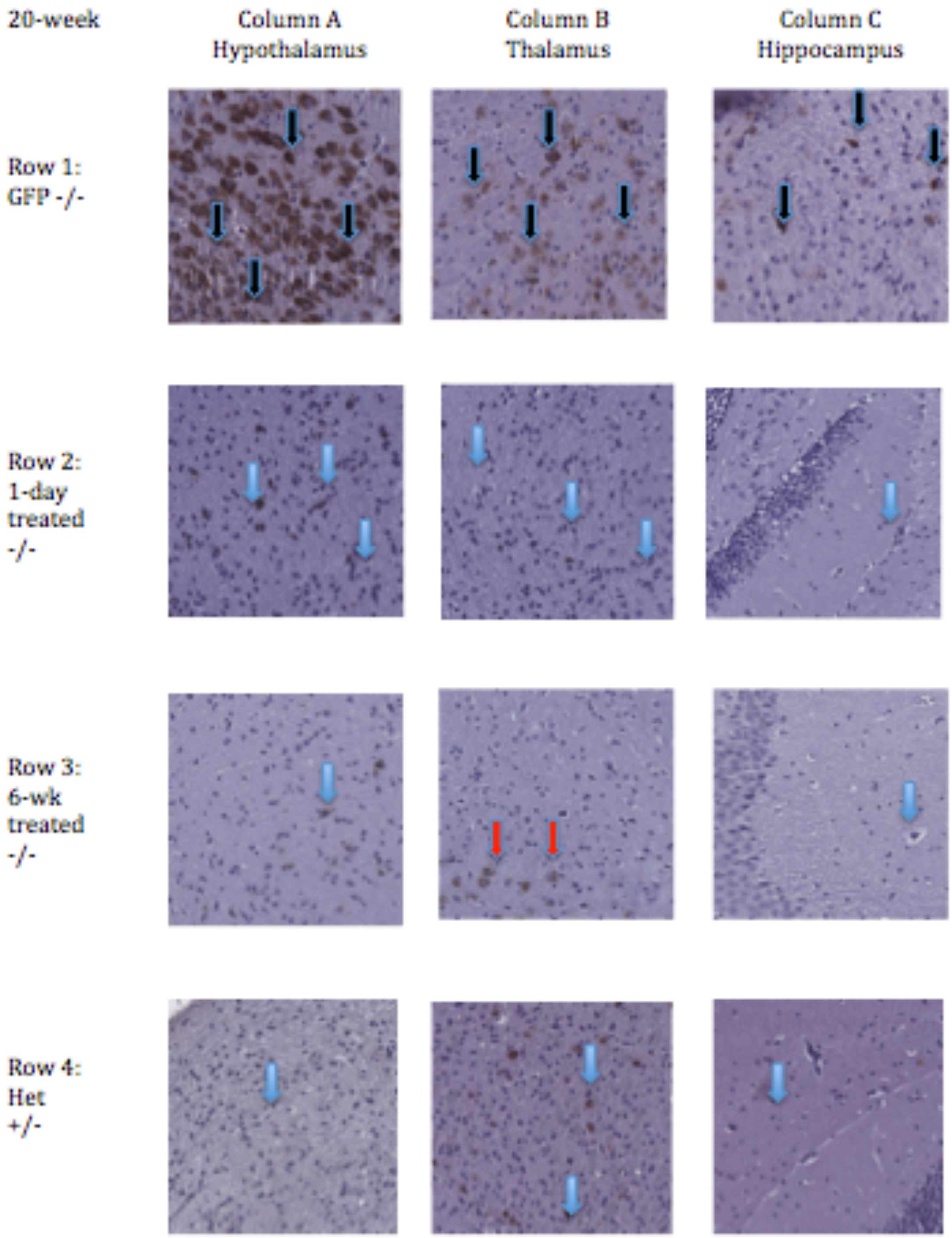

20-week
Column A
Hypothalamus
Column B
Thalamus
Column C
Hippocampus
Row 1:
GFP -/-
Row 2:
1-day
treated
-/-
Row 3:
6-wk
treated
-/-
Row 4:
Het
+/-

B

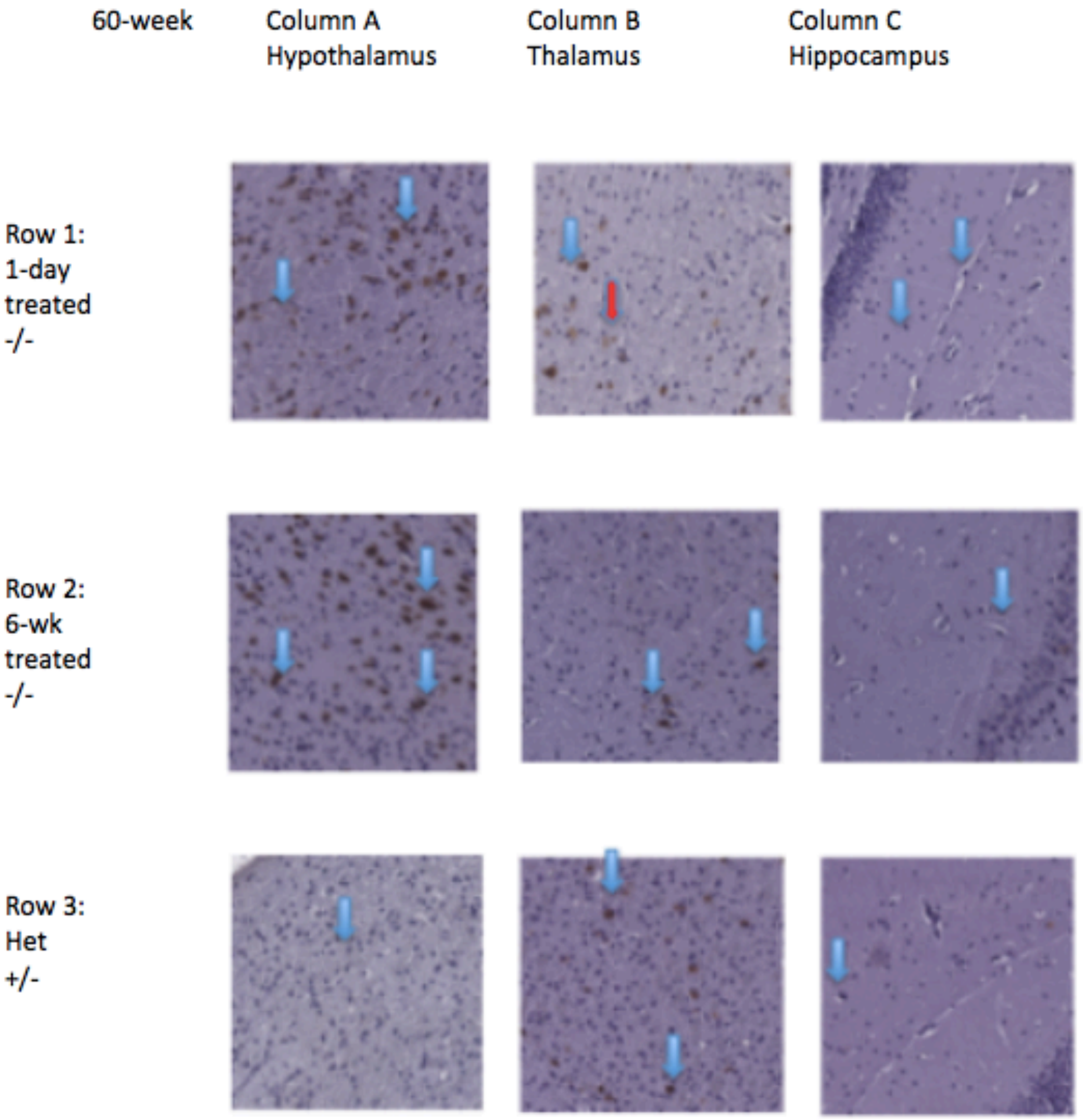
60-week
Column A
Hypothalamus
Column B
Thalamus
Column C
Hippocampus
Row 1:
1-day
treated
-/-
Row 2:
6-wk
treated
-/-
Row 3:
Het
+/-

Figure 11. Histological Ganglioside Storage in the Neurons of 20-week and 60-week Murine Brains

A) Sections of the murine Hypothalamus (Column A), thalamus (Column B), and hippocampus (Column C) from GFP treated (Row 1), neonatal treated (Row 2), adult treated (Row 3) and heterozygous (Row 4) AB- G_{M2} mice.

B) Sections of the murine Hypothalamus (Column A), thalamus (Column B), and hippocampus (Column C) from neonatal treated (Row 1), adult treated (Row 2) and heterozygous (Row 3) AB-G_{M2} mice.

The black arrows depict the G_{M2} ganglioside saturated neurons. The red arrows depict neurons with lesser amounts of G_{M2} ganglioside saturation. The blue arrows depict neuronal nuclei. It seems that the treated mice have less build-up of G_{M2} gangliosides and are similar in build up to the heterozygous mice; with the GFP treated showing the largest amount of G_{M2} ganglioside build up in both the 20- and 60-week cohorts.

Microtome sectioning completed by Karlaina Osmon, PhD candidate in Walia Lab. Histology slides completed by Shakeel Virk and Lee Boudreau from Richardson Labs.

3.3.8 Cohort Weights

Weight measurements were taken for the mice in each cohort, prior to behavioural testing on a monthly basis. The vehicle treated cohorts in both the short- and long-term cohorts were found to have an increase in weight as time progressed when compared to each of the other cohorts (Figure 12A & B).

A

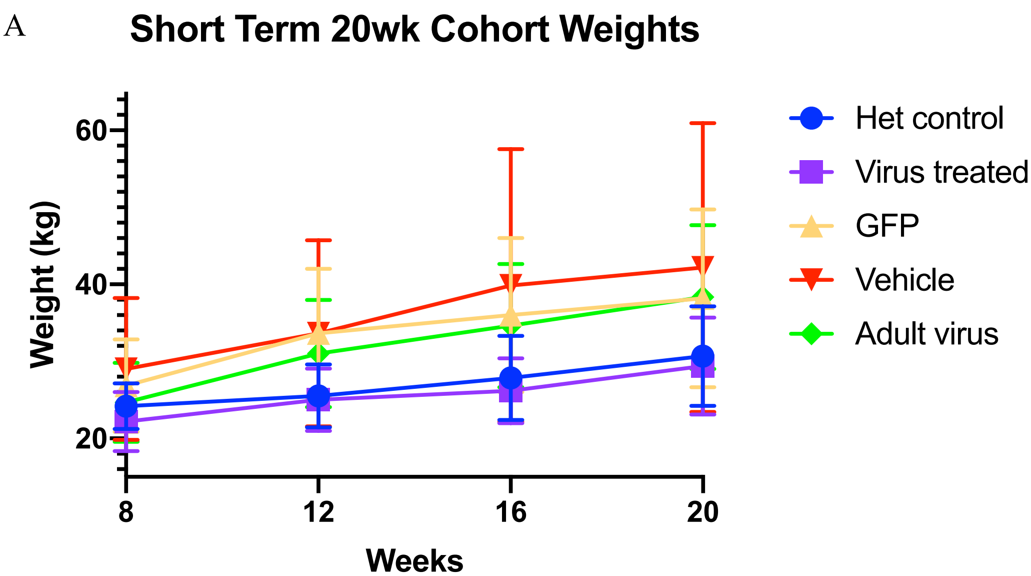

B

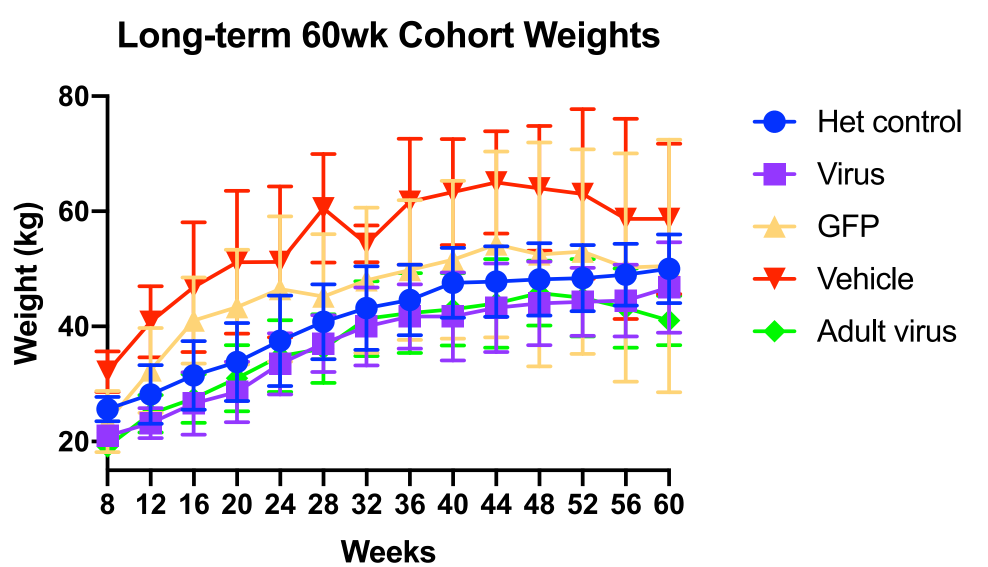

Figure 12. 20-week and 60-week cohort weights. (A)Respective weights at 4-week intervals starting from 8 weeks up to 20 weeks. (B)Respective weights at 4-week intervals starting from 8 weeks up to 60 weeks

3.3.9 Mortality

During the experimental process for the 20wk cohort there was 1 mouse from the 1-day treated cohort that died earlier than the set humane endpoint date. Please refer to Appendix A for further details.

During the experimental process for the 60wk cohort there was 1 mouse from the heterozygous cohort, 2 mice from the 1-day treated cohort, 2 mice from the GFP cohort, 3 mice from the vehicle cohort and 1 mouse from the 6-week treated cohort that died earlier than the set humane endpoint date. Please refer to Appendix B for further details.

Chapter 4

Discussion

4.1 Discussion

This study provides the proof of concept for ssAAV9/*GM2A* to have a therapeutic value in reducing G_{M2} ganglioside accumulation in a mouse model for AB-$_{GM2}$. Our primary outcome measure was to see a reduction of G_{M2} ganglioside storage biochemically within the treated mouse mid-sections in both the short- and long-term cohorts; which we were able to identify. Our secondary outcome measure was to see changes in the treated mouse phenotype in the short- and long-term cohorts through behavioural testing. In the short- and long-term cohorts a single intravenous dose of ssAAV9/*GM2A* did not show a significant improvement in the behavioural results of neonatal and adult virus treated mice. Histological staining showed decreased amounts of G_{M2} ganglioside build-up in the treated groups. Although our study was not able to show statistically significant data both biochemically and phenotypically, it does suggest a therapeutic potential for ssAAV9/*GM2A* to decrease the amount of G_{M2} ganglioside accumulation in an AB-G_{M2} mouse model.

AB-G_{M2} is a progressive neurodegenerative disease. The majority of G_{M2} gangliosides begin to accumulate in the brain and spinal cord prior to any onset of symptoms (Liu et al., 1997). Due to this fact, we decided to inject both neonatal and adult mice. We wanted to elicit whether treating the mice earlier would have a greater impact on decreasing ganglioside build-up compared to treating at a later stage. The rationale behind having a short and long-term cohort was to monitor the effects of treatment in a mouse model with a mild phenotype initially appearing at the 4-5 month period and whether the treatment would delay the onset of symptoms. As the AB-G_{M2} mouse model has normal survival and a milder phenotype it was difficult to discern whether the treatment in the neonate and adult was able to delay the onset of behavioural symptoms. We were able to see some effects of the treated cohorts surpassing the vehicle counterparts in the long term 60-week RR behavioural testing; this was a secondary measure that we were assessing.

The rationale for using GFP as one of the cohorts was two-fold. The GFP cohort behaved as a virus control and partially as a vehicle control because it was able to show us if the AAV9 capsid had any deleterious effects. In our study we were not able to elicit any unwanted effects of the AAV9 capsid injected systemically. Historically, GFP is a marker protein and we would expect to see no effects in the mouse and therefore we did not expect to see any significant changes with using GFP in an AAV9 viral capsid. Due to the intermediate phenotype of our mouse model it did seem at times that the GFP cohort behaved similar to the heterozygous controls. However, since we did not expect to see any behavioural changes until approximately 4-5months of age the GFP could in fact behave as a heterozygous. We were reassured that there was no statistically significant data when comparing the vehicle and GFP treated cohorts. One of the limitations of our study was that we did not include a cohort which included mice that only received the empty AAV9 viral capsid due to its high cost. Whereas, in using GFP in an AAV9 viral capsid; for future studies we would be able to study the GFP immunohistochemistry to assess distribution of the viral vector into various murine organs.

It was a proof-of-concept study and therefore no other studies have shown the effects of systemically introducing ssAAV9/*GM2A* into an AB-G_{M2} mouse model. A comparable dose of treatment was given to our AB-G_{M2} mice in comparison to previously used doses in TSD, SD and other lysosomal storage diseases mouse models (Cachon-Gonzalez et al., 2006; Daly et al., 1999; Miklyaeva et al., 2004; Penati et al., 2017). According to the "critical residual activity threshold" hypothesis (Conzelmann & Sandhoff 1983; Conzelmann & Sandhoff 1987) there should be at least 10% of residual enzyme activity in a lysosomal storage disease mouse model in order for the substrate accumulation to be low enough for the animal to live a normal life (Leinekugel et al., 1992). In recent haemophilia gene therapy study, an increase from <1% of Factor IX expression to 2-6% was sufficient to reach therapeutic benefit (Nathwani et al., 2017). We are not clear what levels are required for GM2AP especially in the brain to be sufficient for therapeutic benefit. In our study although there was no deficiency in the HexA or HexB enzymes; there was a deficiency of the GM2AP, which acts as a co-factor to allow for the degradation of G_{M2} gangliosides. Though difficult to assess, it appears we may have been able to reach the required critical threshold level in our study through some improvement in behavioural testing and a reduction in G_{M2} ganglioside storage biochemically in the 20- and 60-week cohorts.

Vector biodistribution analysis was used to determine the effectiveness of the ssAAV9/*GM2A* therapy. The biodistribution was able to show that the vector therapy was able to cross the BBB and vector copies were detectable throughout the caudal section, rostral section and mid-section. The vector copy number in the liver was high in comparison to the brain as expected and similar to that seen in other studies (Osmon et al., 2016, Walia et al., 2015). The liver was shown to have greater biodistribution in comparison to other areas of the brain. This study did not focus on dosage optimization; but in other studies, it was seen that with higher dosages the copy number in the brain increased (Cachon-Gonzalez et al., 2006; Walia et al., 2015). However, many studies also used various vector types, which also makes it difficult to compare to our study (Arfi et al., 2005; Bourgoin et al., 2003; Kyrkanides et al., 2005; Martino et al., 2005). Analysis of GM2AP expression was also done by western blot, which confirmed that the correct sized protein of interest was expressed in the adult treated mouse liver sample.

There was a decrease in the G_{M2} ganglioside storage seen in both the 20-week and 60-week cohorts (see Figure 9). In the 20-week cohort there was a significant decrease in the amount of G_{M2} ganglioside storage in the mid-sections of the 1-day old and 6-week ssAAV9/*GM2A* treated cohorts when compared to the vehicle KO group, respectively. The 60-week cohort showed a decrease in ganglioside storage for both the 1-day and 6-week treated groups in comparison to the vehicle KO group; however this decrease was not statistically significant (see Figure 9). Both cohorts were euthanized using the same protocol and methods. This may indicate that the dose was not sufficient to keep the build-up lower for a long period of time. This could possibly be due to an immune response depleting the transduced number of cells over time.

Behavioural testing in previous studies have shown that overall RR performance in the KO group was significantly impaired in comparison to the control groups (Liu et al., 1997). These studies also demonstrated the control groups as having a significant improvement in performance on the rotarod over a 20-week period. Our data for the RR short-term 20-week time point did not show statistically significant data in comparison to the vehicle cohort (see Figure 6D, E, F). Previous studies also showed that in the OFT there was no significant difference between the KO groups and control groups over a 20-week time course (Liu et al., 1997). In our study we saw similar results in both the 20- and 60-week cohorts (Figure 6A-C & 7A-C). It is difficult to interpret the data for the OFT as not all the data had significant ANOVA results and performing so many ANOVA's and multiple comparisons would eventually produce statistically significant data. The muscular strength test at 20-and 60-weeks did not show a statistically significant difference between the treated and control cohorts compared to the vehicle KO groups (see Figure 8). Behavioural testing was able to show its main significant effects on time, where with increasing age of the mice, the behavioural signs and symptoms worsened, and performance declined.

Histologically, the 20-week cohort as well as the 60-week cohort showed decreased accumulation of G_{M2} gangliosides when compared to the untreated/GFP group (see Figure 11). The build-up in both treated cohorts is similar to that of the heterozygous group. A previous study showed that even though the pathological process worsened in the various treated and untreated groups with age, the biodistribution of the G_{M2} ganglioside storage was similar regardless of age (Liu et al., 1997). A previous study also showed that there was substantial build-up of G_{M2} gangliosides in the hypothalamic nuclei (Liu et al., 1997). We could see a large build-up of the G_{M2} gangliosides in the untreated GFP group in our histology staining; with a reduced build-up in the neonatal and adult treated groups at both 20- and 60-week end points (see Figure 11).

Lung as well as liver tumors have been noted in previous studies that used AAV vectors as a potential treatment in neonate pups (Bell et al., 2006, Russell, 2007; Walia et al., 2015). This study did not have any tumor development noted in any of the harvested organs at either 20- or 60-week end points. The mechanism behind tumor formation with AAV viral vectors is currently not well understood, but postulated to be due to integration of vector sequences close to tumour suppressor genes or proto-oncogenes. Previous studies had used a larger dose, which may have contributed to the tumor formation; however our use of a lower dose of ssAAV9/*GM2A* may contribute to why we were not able to encounter any tumour formation.

4.2 Limitations

In scientific studies there are always limitations, which could further progress the scientific findings if implemented in future studies. In our study the difference in phenotype seen in a mouse model compared to a human would serve to be the main limitation (Phaneuf et al., 1996). Since the AB-G_{M2} mouse model has a weak/intermediate phenotype it was unable to mimic the actual human disease state in its infantile stage but is close to adult-onset disease. There is a difference biochemically in terms of the degradative pathways of G_{M2} gangliosides in a mouse model as opposed to a human. In humans, there is only one degradative pathway in which G_{M2} is degraded by HexA in its entirety (Bertoni et al., 1999; Yuziuk et al., 1998). This is the reason why being deficient in the *HEX A* gene (known as TSD) leads to a large build-up of G_{M2} gangliosides within the brain and spinal cord in a human (Lawson CA, Martin DR. 2016). In mice there are two degradative pathways, which allow for some slower residual activity to catabolize G_{M2} gangliosides as well (Liu et al., 1997). Of the three Hex isozymes, HexA is the only isozyme that has an interaction with GM2AP (Tropak et al., 2016). The efficacy of the ssAAV9/*GM2A* administration in a human with AB-G_{M2} might give significantly different results if there is only one pathway able to degrade G_{M2} gangliosides in humans.

Confounding variables that affected our study were the fact that there was a loss of animals over the duration of the study. Our sample size per cohort was 6. We did have cohorts where the mice would not live up to their pre-determined endpoint and died due to unknown causes. This created a smaller sample size for our study, a smaller 'n.' Power would become lower and therefore our study would have lower confidence levels. This results in a lower probability of finding a statistically significant difference between the cohorts.

In our statistical analyses, due to the multiple ANOVA's done for the different behavioural testing parameters and the various comparisons between each of the cohorts our multiple comparisons tests did show various cohorts where there was a statistically significant difference between the treated and untreated cohorts. However, this data should be interpreted cautiously as not all of our ANOVA studies showed statistically significant data; and yet we still conducted multiple comparisons tests for those data sets. Technically, multiple comparisons tests would not be done after finding no significance in the ANOVA to begin with. Essentially, if you complete a specific statistical analysis enough times; there will be some statistically significant data that will be found, and it is difficult to interpret whether this is due to chance alone or whether the value is indeed statistically significant.

The effect of habituation is also a cofounding variable for one of the behavioural measures, the open field test. The open field test is meant to measure general locomotion. However, it is known that when mice are placed in a new environment they explore for a period of time and then their level of exploration decreases (Bolivar 2009). This is known as habituation. The cognitive map theory (O'Keefe and Nadel, 1978) states that when a new environment is explored by an organism, an internal map is created in the hippocampus; and as this environment is frequented more often this internal map becomes more complete, thus reducing exploration (O'Keefe and Nadel, 1978). The effects of habituation make it difficult to assess whether the mice had decreased locomotion due to a lack of GM2AP or whether they were habituated to the OFT over time. There was also a considerable amount of weight gain seen in the vehicle cohorts at both time points. We were unable to determine why this particular cohort showed an increase in weight with time and no prior studies have attributed a lack of GM2AP to increased weight or obesity. This would also have an effect on the OFT as general locomotion may have been reduced in this cohort due to increase in weight.

There was no method of randomization used when delivering virus, vehicle, or GFP to the experimental animals because there was no effective method of distinguishing one pup from the next in a cage at 1 day of age. We also had 2 cohorts within the short- and long-term cohorts where the pups all came from the same dam. Therefore, there was no randomization of dams for all of the cohorts. Ideally, we would want to have mice from different litters, and therefore dams, within each cohort so that there would not be a dam effect on the litter produced and we could account for the potential of any genetic or neurobiological effects that the dam may have on one particular litter of pups. For example is the dam as predisposed to weight gain, her pups may have also grown to be overweight.

Short-term histology staining included a control group, which was the GFP treated group. However, the long-term histology staining did not have a true control group as there were no 6-week adult injected mice with GFP. To implement this in the future, having a well identified adult GFP control would be ideal to compare to the treated cohorts. We were unable to successfully section usable sections of the mouse cerebellum for histological staining. As the phenotypic and pathological changes occur mainly in the cerebellum it is difficult to extrapolate what we could have found if we were able to stain and visualize the cerebellar section of the mouse brain.

General locomotion was tested in the open field test; however, the fact that the untreated vehicle and GFP groups had major weight gain with increasing age adds a confounding variable to testing general locomotion, motor coordination and muscular strength in a mouse model. It is difficult to assess whether the mice had decreased locomotion; changes in motor coordination and muscular strength due to a lack of GM2AP or whether they were not as mobile; coordinated or strong due to their considerable weight gain. The decreased activity in the vehicle and GFP mice could likely be sufficient to account for the considerable amount of weight gain we saw in that cohort.

In using viral vectors one also has to be aware of the potential for side effects from therapy. We have come a long way from the initial human clinical trials posing extensive risks, such as malignancies, as well as one case ending up in a lethal outcome (Marshall E. 1999; Thomas CE, Ehrhardt A, and Kay MA. 2003). There has been tumorigenesis seen in previous studies using AAV vectors in treating mucopolysaccharidosis, Sandhoff disease, β-glucuronidase deficiency and OTC deficiencies (Donsante et al., 2001; Ruzo et al., 2012; Zhong et al., 2013; Walia et al., 2015). At least one of these studies showing tumorigenesis did use larger doses than our study, which may be one of the contributing factors as to why our study did not show any tumour formation (Donsante et al., 2007; Russell 2007; Walia et al., 2015; Wang et al., 2012).

4.3 Future Direction

Future research should focus not only on the primary, but also secondary factors contributing to the pathogenesis of G_{M2} gangliosidoses (Gabig-Ciminska et al., 2015; Hawkins-Salsbury et al., 2011; Macauley 2016; Vitner et al., 2010). One of the trademark pathologies seen in progressive CNS disease states, especially G_{M2} Gangliosidoses, is an increased inflammatory response (Abo-Ouf et al., 2013; Cachon-Gonazalez et al., 2014). Previous studies done in a murine model for SD showed microglial activation prior to any subtle neurodegeneration (Cachon-Gonzalez et al., 2014; Wada et al., 2000). Our lab has already started a project analyzing the immune response in G_{M2} gangliosidoses murine models to assess whether pre-treating with an anti-inflammatory agent decreases the immune response, which tends to develop after AAV vector therapy administration. We hope to see a positive outcome from this initiative.

Further research is required to look into the implementation of different dosages of viral vector therapy in an AB-G_{M2} murine model. As we used a comparable dose in comparison to similar research done by other researchers (Conzelmann & Sandhoff 1983; Walia et al., 2015), a higher dose may scale up the benefits we saw in our study. In addition, we could then use a combination of a higher therapeutic dose along with tackling a secondary mechanism to analyze the results of G_{M2} ganglioside accumulation and behavioural effects (Hawkins-Salsbury et al., 2011).

4.4 Conclusion

The goal of this proof-of-concept study was to use the least invasive method to assess the therapeutic value of introducing an AAV-vector containing *GM2A* into an AB-G_{M2} murine model; and to assess its efficacy. We achieved our primary outcome of G_{M2} ganglioside reduction seen biochemically in both the short- and long-term cohorts. Our study showed our short- and long-term treated cohorts inconsistently outperformed their untreated counterparts (vehicle, KO) cohorts in the majority of the behavioural testing methods. We also saw a decrease in the G_{M2} ganglioside build-up through histological analysis in our short- and long-term cohorts of neonatal and adult treated mice. We did see persistence of the vector for long-term testing within the liver and the rostral section, caudal section and mid sections of the murine brain in both short- and long-term cohorts. The outcomes of our study are able to aid in developing a potential therapeutic strategy for AB-G_{M2} and the results can be extended to other neurodegenerative diseases, some of which are only being treated by palliative care at this time.

Bibliography

Abo-ouf, H. *et al.* Deletion of tumor necrosis factor-α ameliorates neurodegeneration in Sandhoff disease mice. *Hum Mol Genet* **22**, 3960–3975 (2013).

Arfi, A., Bourgoin, C., Basso, L., Emiliani, C., Tancini, B., Chigorno, V., … Caillaud, C. (2005). Bicistronic lentiviral vector corrects beta-hexosaminidase deficiency in transduced and cross-corrected human Sandhoff fibroblasts. *Neurobiology of Disease*, *20*(2), 583–593. https://doi.org/10.1016/j.nbd.2005.04.017

Assessment of adenoviral vector safety and toxicity: report of the National Institutes of Health Recombinant DNA Advisory Committee. (2002). *Human Gene Therapy*, *13*(1), 3–13. https://doi.org/10.1089/10430340152712629

Bell, P. *et al.* Analysis of tumors arising in male B6C3F1 mice with and without AAV vector delivery to liver. *Mol. Ther.* **14**, 34–44 (2006).

Benkhelifa-Ziyyat, S., Besse, A., Roda, M., Duque, S., Astord, S., Carcenac, R., … Barkats, M. (2013). Intramuscular scAAV9-SMN injection mediates widespread gene delivery to the spinal cord and decreases disease severity in SMA mice. *Molecular Therapy: The Journal of the American Society of Gene Therapy*, *21*(2), 282–290. https://doi.org/10.1038/mt.2012.261

Bertoni, C., Li, Y. T. & Li, S. C. Catabolism of asialo-GM2 in man and mouse. Specificity of human/mouse chimeric GM2 activator proteins. *J. Biol. Chem.* **274**, 28612–28618 (1999).

Blaese, R. M., Culver, K. W., Miller, A. D., Carter, C. S., Fleisher, T., Clerici, M., … Anderson, W. F. (1995). T lymphocyte-directed gene therapy for ADA- SCID: initial trial results after 4 years. *Science (New York, N.Y.)*, *270*(5235), 475–480.

Boelens, J. J. (2006). Trends in haematopoietic cell transplantation for inborn errors of metabolism. *Journal of Inherited Metabolic Disease*, *29*(2-3), 413–420. https://doi.org/10.1007/s10545-005-0258-8

Bolivar, V. J. Intrasession and Intersession Habituation in Mice: From Inbred Strain Variability to Linkage Analysis. *Neurobiol Learn Mem* **92**, 206–214 (2009).

Bourgoin, C. *et al.* Widespread distribution of beta-hexosaminidase activity in the brain of a Sandhoff mouse model after coinjection of adenoviral vector and mannitol. *Gene Ther.* **10**, 1841–1849 (2003).

Cachón-González, M. B., Wang, S. Z., Lynch, A., Ziegler, R., Cheng, S. H., & Cox, T. M. (2006). Effective gene therapy in an authentic model of Tay-Sachs-related diseases. *Proceedings of the National Academy of Sciences of the United States of America*, *103*(27), 10373–10378. https://doi.org/10.1073/pnas.0603765103

Cachón-González, M.-B., Wang, S. Z., Ziegler, R., Cheng, S. H., & Cox, T. M. (2014). Reversibility of neuropathology in Tay-Sachs-related diseases. *Human Molecular Genetics*, *23*(3), 730–748. https://doi.org/10.1093/hmg/ddt459

Clarke, L. A., & Hollak, C. E. M. (2015). The clinical spectrum and pathophysiology of skeletal complications in lysosomal storage disorders. *Best Practice & Research. Clinical Endocrinology & Metabolism*, *29*(2), 219–235. https://doi.org/10.1016/j.beem.2014.08.010

Conzelmann, E., Sandhoff, K., Nehrkorn, H., Geiger, B. & Arnon, R. Purification, biochemical and immunological characterisation of hexosaminidase A from variant AB of infantile GM2 gangliosidosis. *Eur. J. Biochem.* **84**, 27–33 (1978).

Conzelmann, E., & Sandhoff, K. (1979). Purification and characterization of an activator protein for the degradation of glycolipids GM2 and GA2 by hexosaminidase A. *Hoppe-Seyler's Zeitschrift Fur Physiologische Chemie*, *360*(12), 1837–1849.

Conzelmann, E., & Sandhoff, K. (1983). Partial enzyme deficiencies: residual activities and the development of neurological disorders. *Developmental Neuroscience*, *6*(1), 58–71. https://doi.org/10.1159/000112332

Conzelmann, E., & Sandhoff, K. (1987). Activator proteins for lysosomal glycolipid hydrolysis. *Methods in Enzymology*, *138*, 792–815.

Coura, R. dos S., & Nardi, N. B. (2007). The state of the art of adeno-associated virus-based vectors in gene therapy. *Virology Journal*, *4*, 99. https://doi.org/10.1186/1743-422X-4-99

Cox, T., Lachmann, R., Hollak, C., Aerts, J., van Weely, S., Hrebícek, M., … Zimran, A. (2000). Novel oral treatment of Gaucher's disease with N-butyldeoxynojirimycin (OGT 918) to decrease substrate biosynthesis. *Lancet (London, England)*, *355*(9214), 1481–1485. https://doi.org/10.1016/S0140-6736(00)02161-9

Daly, T. M., Vogler, C., Levy, B., Haskins, M. E., & Sands, M. S. (1999). Neonatal gene transfer leads to widespread correction of pathology in a murine model of lysosomal storage disease. *Proceedings of the National Academy of Sciences of the United States of America*, *96*(5), 2296–2300.

Donsante, A., Miller, D. G., Li, Y., Vogler, C., Brunt, E. M., Russell, D. W., & Sands, M. S. (2007). AAV vector integration sites in mouse hepatocellular carcinoma. *Science (New York, N.Y.)*, *317*(5837), 477. https://doi.org/10.1126/science.1142658

Donsante, A., Vogler, C., Muzyczka, N., Crawford, J. M., Barker, J., Flotte, T., … Sands, M. S. (2001). Observed incidence of tumorigenesis in long-term rodent studies of rAAV vectors. *Gene Therapy*, *8*(17), 1343–1346. https://doi.org/10.1038/sj.gt.3301541

Duque, S., Joussemet, B., Riviere, C., Marais, T., Dubreil, L., Douar, A.-M., … Barkats, M. (2009). Intravenous Administration of Self-complementary AAV9 Enables Transgene Delivery to Adult Motor Neurons. *Molecular Therapy: The Journal of the American Society of Gene Therapy*, *17*(7), 1187–1196. https://doi.org/10.1038/mt.2009.71

Ferrari, F. K., Samulski, T., Shenk, T., & Samulski, R. J. (1996). Second-strand synthesis is a rate-limiting step for efficient transduction by recombinant adeno-associated virus vectors. *Journal of Virology*, *70*(5), 3227–3234.

Ferreira, C. R., & Gahl, W. A. (n.d.). Lysosomal storage diseases. *Translational Science of Rare Diseases*, *2*(1-2), 1–71. https://doi.org/10.3233/TRD-160005

Fisher, K. J., Gao, G. P., Weitzman, M. D., DeMatteo, R., Burda, J. F., & Wilson, J. M. (1996). Transduction with recombinant adeno-associated virus for gene therapy is limited by leading-strand synthesis. *Journal of Virology*, *70*(1), 520–532.

Folch, J., Ascoli, I., Lees, M., Meath, J.A., & LeBaron, F.N. (1951). Preparation of Lipide Extracts from Brain Tissue. *Journal of Biological Chemistry*, 191(2), 833-841.

Foust, K. D., Nurre, E., Montgomery, C. L., Hernandez, A., Chan, C. M., & Kaspar, B. K. (2009a). Intravascular AAV9 preferentially targets neonatal neurons and adult astrocytes. *Nature Biotechnology*, *27*(1), 59–65. https://doi.org/10.1038/nbt.1515

Foust, K. D., Nurre, E., Montgomery, C. L., Hernandez, A., Chan, C. M., & Kaspar, B. K. (2009b). Intravascular AAV9 preferentially targets neonatal-neurons and adult-astrocytes in CNS. *Nature Biotechnology*, *27*(1), 59–65. https://doi.org/10.1038/nbt.1515

Gabig-Cimińska, M., Jakóbkiewicz-Banecka, J., Malinowska, M., Kloska, A., Piotrowska, E., Chmielarz, I., … Węgrzyn, G. (2015). Combined Therapies for Lysosomal Storage Diseases. *Current Molecular Medicine*, *15*(8), 746–771.

Ginn, S. L., Amaya, A. K., Alexander, I. E., Edelstein, M., & Abedi, M. R. (n.d.). Gene therapy clinical trials worldwide to 2017: An update. *The Journal of Gene Medicine*, *20*(5), e3015. https://doi.org/10.1002/jgm.3015

Gravel R, Kaback MM et al (2014) The GM2 Gangliosidoses. In: Valle D, Vogelstein B, Kinzler KW, Antonarakis SE, Ballabio A, Gibson K, Mitchell G (eds) OMMBID. McGraw-Hill, New York

Gruenert, A. K., Czugala, M., Mueller, C., Schmeer, M., Schleef, M., Kruse, F. E., & Fuchsluger, T. A. (2016). Self-Complementary Adeno-Associated Virus Vectors Improve Transduction Efficiency of Corneal Endothelial Cells. *PloS One*, *11*(3), e0152589. https://doi.org/10.1371/journal.pone.0152589

Hardcastle, N., Boulis, N. M., & Federici, T. (2018). AAV gene delivery to the spinal cord: serotypes, methods, candidate diseases, and clinical trials. *Expert Opinion on Biological Therapy*, *18*(3), 293–307. https://doi.org/10.1080/14712598.2018.1416089

Hawkins-Salsbury, J. A., Reddy, A. S., & Sands, M. S. (2011). Combination therapies for lysosomal storage disease: is the whole greater than the sum of its parts? *Human Molecular Genetics*, *20*(R1), R54–R60. https://doi.org/10.1093/hmg/ddr112

Hollak, C. E. M., & Wijburg, F. A. (2014). Treatment of lysosomal storage disorders: successes and challenges. *Journal of Inherited Metabolic Disease*, *37*(4), 587–598. https://doi.org/10.1007/s10545-014-9718-3

Jarnes Utz, J. R., Kim, S., King, K., Ziegler, R., Schema, L., Redtree, E. S., & Whitley, C. B. (2017). Infantile gangliosidoses: Mapping a timeline of clinical changes. *Molecular Genetics and Metabolism*, *121*(2), 170–179.https://doi.org/10.1016/j.ymgme.2017.04.011

Jeyakumar, M., Butters, T. D., Cortina-Borja, M., Hunnam, V., Proia, R. L., Perry, V. H., …

Platt, F. M. (1999). Delayed symptom onset and increased life expectancy in Sandhoff disease mice treated with N-butyldeoxynojirimycin. *Proceedings of the National Academy of Sciences of the United States of America*, *96*(11), 6388–6393.

John O'Keefe & Lynn Nadel (1978) *The Hippocampus as a Cognitive Map*, Oxford University Press.

JoVE | Peer Reviewed Scientific Video Journal - Methods and Protocols. (n.d.). Retrieved July 23, 2018, from https://www.jove.com/trialform?type=subscription

Kafri, T., Morgan, D., Krahl, T., Sarvetnick, N., Sherman, L., & Verma, I. (1998). Cellular immune response to adenoviral vector infected cells does not require de novo viral gene expression: implications for gene therapy. *Proceedings of the National Academy of Sciences of the United States of America*, *95*(19), 11377–11382.

Kay, M. A., Glorioso, J. C. & Naldini, L. Viral vectors for gene therapy: the art of turning infectious agents into vehicles of therapeutics. *Nat. Med.* **7**, 33–40 (2001).

Krivit, W., Peters, C., & Shapiro, E. G. (1999). Bone marrow transplantation as effective treatment of central nervous system disease in globoid cell leukodystrophy, metachromatic leukodystrophy, adrenoleukodystrophy, mannosidosis, fucosidosis, aspartylglucosaminuria, Hurler, Maroteaux-Lamy, and Sly syndromes, and Gaucher disease type III. *Current Opinion in Neurology*, *12*(2), 167–176.

Kolter, T. & Sandhoff, K. Principles of lysosomal membrane digestion: stimulation of sphingolipid degradation by sphingolipid activator proteins and anionic lysosomal lipids. *Annu. Rev. Cell Dev. Biol.* **21**, 81–103 (2005).

Kolter, T. & Sandhoff, K. Sphingolipid metabolism diseases. *Biochimica et Biophysica*

Acta (BBA) - Biomembranes **1758**, 2057–2079 (2006).

Kyrkanides, S., Miller, J. H., Brouxhon, S. M., Olschowka, J. A. & Federoff, H. J. beta-hexosaminidase lentiviral vectors: transfer into the CNS via systemic administration. *Brain Res. Mol. Brain Res.* **133**, 286–298 (2005).

Lawson, C. A., & Martin, D. R. (2016). Animal models of GM2 gangliosidosis: utility and limitations. *The Application of Clinical Genetics*, *9*, 111–120. https://doi.org/10.2147/TACG.S85354

Leinekugel, P., Michel, S., Conzelmann, E., & Sandhoff, K. (1992). Quantitative correlation between the residual activity of beta-hexosaminidase A and arylsulfatase A and the severity of the resulting lysosomal storage disease. *Human Genetics*, *88*(5), 513–523.

Lewandoski, M. (2001). Conditional control of gene expression in the mouse. *Nature Reviews. Genetics*, *2*(10), 743–755. https://doi.org/10.1038/35093537

Liu, Y., Hoffmann, A., Grinberg, A., Westphal, H., McDonald, M. P., Miller, K. M., … Proia, R. L. (1997). Mouse model of GM2 activator deficiency manifests cerebellar pathology and motor impairment. *Proceedings of the National Academy of Sciences of the United States of America*, *94*(15), 8138–8143.

Li, Y., & Sands, M. S. (2014). Experimental therapies in the murine model of globoid cell leukodystrophy. *Pediatric Neurology*, *51*(5), 600–606. https://doi.org/10.1016/j.pediatrneurol.2014.08.003

Lo, W. D., Qu, G., Sferra, T. J., Clark, R., Chen, R., & Johnson, P. R. (1999). Adeno-associated virus-mediated gene transfer to the brain: duration and modulation of expression. *Human Gene Therapy*, *10*(2), 201–213. https://doi.org/10.1089/10430349950018995

Macauley, S. L. (2016). Combination Therapies for Lysosomal Storage Diseases: A Complex

Answer to a Simple Problem. *Pediatric Endocrinology Reviews: PER*, *13 Suppl 1*, 639–648.

Maegawa, G. H. B., Banwell, B. L., Blaser, S., Sorge, G., Toplak, M., Ackerley, C., … Clarke, J. T. R. (2009). Substrate reduction therapy in juvenile GM2 gangliosidosis. *Molecular Genetics and Metabolism*, *98*(1-2), 215–224. https://doi.org/10.1016/j.ymgme.2009.06.005

Mahuran, D. J. (1998). The GM2 activator protein, its roles as a co-factor in GM2 hydrolysis and as a general glycolipid transport protein. *Biochimica Et Biophysica Acta*, *1393*(1), 1–18.

Mahuran, D. J. (1999). Biochemical consequences of mutations causing the GM2 gangliosidoses. *Biochimica Et Biophysica Acta*, *1455*(2-3), 105–138.

Malatack, J. J., Consolini, D. M., & Bayever, E. (2003). The status of hematopoietic stem cell transplantation in lysosomal storage disease. *Pediatric Neurology*, *29*(5), 391–403.

Marshall, E. (1999). Gene therapy death prompts review of adenovirus vector. *Science (New York, N.Y.)*, *286*(5448), 2244–2245.

Martin, D. R., Cox, N. R., Morrison, N. E., Kennamer, D. M., Peck, S. L., Dodson, A. N., … Baker, H. J. (2005). Mutation of the GM2 activator protein in a feline model of GM2 gangliosidosis. *Acta Neuropathologica*, *110*(5), 443–450. https://doi.org/10.1007/s00401-005-1040-6

Martino, S., Marconi, P., Tancini, B., Dolcetta, D., De Angelis, M. G. C., Montanucci, P., … Orlacchio, A. (2005). A direct gene transfer strategy via brain internal capsule reverses the biochemical defect in Tay-Sachs disease. *Human Molecular Genetics*, *14*(15), 2113–2123. https://doi.org/10.1093/hmg/ddi216

Mathias, J. D., Ran, Y., Carter, J. D., & Fanucci, G. E. (2009). Interactions of the GM2 Activator

Protein with Phosphatidylcholine Bilayers: A Site-Directed Spin-Labeling Power Saturation Study. *Biophysical Journal*, *97*(5), 1436–1444. https://doi.org/10.1016/j.bpj.2009.05.058

McCarty, D. M. (2008). Self-complementary AAV vectors; advances and applications. *Molecular Therapy: The Journal of the American Society of Gene Therapy*, *16*(10), 1648–1656. https://doi.org/10.1038/mt.2008.171

McCarty, D. M., Monahan, P. E., & Samulski, R. J. (2001). Self-complementary recombinant adeno-associated virus (scAAV) vectors promote efficient transduction independently of DNA synthesis. *Gene Therapy*, *8*(16), 1248–1254. https://doi.org/10.1038/sj.gt.3301514

McCown, T. J. (2011). Adeno-Associated Virus (AAV) Vectors in the CNS. *Current Gene Therapy*, *11*(3), 181–188.

Merkel, S. F. *et al.* Trafficking of AAV vectors across a model of the blood-brain barrier; a comparative study of transcytosis and transduction using primary human brain endothelial cells. *J Neurochem* **140**, 216–230 (2017).

Miklyaeva, E. I., Dong, W., Bureau, A., Fattahie, R., Xu, Y., Su, M., … Gravel, R. A. (2004). Late onset Tay-Sachs disease in mice with targeted disruption of the Hexa gene: behavioral changes and pathology of the central nervous system. *Brain Research*, *1001*(1-2), 37–50. https://doi.org/10.1016/j.brainres.2003.11.067

Morsy, M. A. & Caskey, C. T. Expanded-capacity adenoviral vectors--the helper-dependent vectors. *Mol Med Today* **5**, 18–24 (1999).

Naso, M. F., Tomkowicz, B., Perry, W. L. & Strohl, W. R. Adeno-Associated Virus (AAV) as a Vector for Gene Therapy. *BioDrugs* **31**, 317–334 (2017).

Nathwani, A. C., Davidoff, A. M. & Tuddenham, E. G. D. Gene Therapy for Hemophilia.

Hematol. Oncol. Clin. North Am. **31**, 853–868 (2017).

Okada, S. & O'Brien, J. S. Tay-Sachs disease: generalized absence of a beta-D-N-acetylhexosaminidase component. *Science* **165**, 698–700 (1969).

Osmon, K. J. L., Woodley, E., Thompson, P., Ong, K., Karumuthil-Melethil, S., Keimel, J. G., … Walia, J. S. (2016). Systemic Gene Transfer of a Hexosaminidase Variant Using an scAAV9.47 Vector Corrects GM2 Gangliosidosis in Sandhoff Mice. *Human Gene Therapy*, *27*(7), 497–508. https://doi.org/10.1089/hum.2016.015

Penati, R., Fumagalli, F., Calbi, V., Bernardo, M. E., & Aiuti, A. (2017). Gene therapy for lysosomal storage disorders: recent advances for metachromatic leukodystrophy and mucopolysaccaridosis I. *Journal of Inherited Metabolic Disease*, *40*(4), 543–554. https://doi.org/10.1007/s10545-017-0052-4

Phaneuf, D., Wakamatsu, N., Huang, J. Q., Borowski, A., Peterson, A. C., Fortunato, S. R., … Gravel, R. A. (1996). Dramatically different phenotypes in mouse models of human Tay-Sachs and Sandhoff diseases. *Human Molecular Genetics*, *5*(1), 1–14.

Platt, F. M., & Lachmann, R. H. (2009). Treating lysosomal storage disorders: current practice and future prospects. *Biochimica Et Biophysica Acta*, *1793*(4), 737–745. https://doi.org/10.1016/j.bbamcr.2008.08.009

Potprommanee, L., Ma, H.-T., Chen, C.-H., Aobchey, P., Boonyapranai, K., Chewaskulyong, B., … Chen, S.-T. (2013). Human Urinary GM2-activator Protein as a Potential Biomarker for Lung Cancer. *Journal of Proteomics & Bioinformatics*, *6*(11). https://doi.org/10.4172/jpb.1000289

Renaud, D., & Brodsky, M. (2016). GM2-Gangliosidosis, AB Variant: Clinical, Ophthalmological, MRI, and Molecular Findings. *JIMD Reports*, *25*, 83–86. https://doi.org/10.1007/8904_2015_469

Rigat, B., Yeger, H., Shehnaz, D., & Mahuran, D. (2009). GM2 activator protein inhibits platelet activating factor signaling in rats. *Biochemical and Biophysical Research Communications*, *385*(4), 576–580. https://doi.org/10.1016/j.bbrc.2009.05.116

Russell, D. W. (2007). AAV vectors, insertional mutagenesis, and cancer. *Molecular Therapy: The Journal of the American Society of Gene Therapy*, *15*(10), 1740–1743. https://doi.org/10.1038/sj.mt.6300299

Ruzo, A., Marcó, S., García, M., Villacampa, P., Ribera, A., Ayuso, E., … Bosch, F. (2012). Correction of pathological accumulation of glycosaminoglycans in central nervous system and peripheral tissues of MPSIIIA mice through systemic AAV9 gene transfer. *Human Gene Therapy*, *23*(12), 1237–1246. https://doi.org/10.1089/hum.2012.029

Sandhoff, K., & Harzer, K. (2013). Gangliosides and gangliosidoses: principles of molecular and metabolic pathogenesis. *The Journal of Neuroscience: The Official Journal of the Society for Neuroscience*, *33*(25), 10195–10208. https://doi.org/10.1523/JNEUROSCI.0822-13.2013

Sandhoff, K., & Kolter, T. (2003). Biosynthesis and degradation of mammalian glycosphingolipids. *Philosophical Transactions of the Royal Society B: Biological Sciences*, *358*(1433), 847–861. https://doi.org/10.1098/rstb.2003.1265

Sandhoff, K. & Kolter, T. Biosynthesis and degradation of mammalian glycosphingolipids. *Philos. Trans. R. Soc. Lond., B, Biol. Sci.* **358**, 847–861 (2003).

Sandhoff, K. The biochemistry of sphingolipid storage diseases. *Angew. Chem. Int. Ed. Engl.* **16**, 273–285 (1977).

Shin, J., Kim, G., Lee, J. W., Lee, J. E., Kim, Y. S., Yu, J.-H., … Lee, C. (2016). Identification of ganglioside GM2 activator playing a role in cancer cell migration through proteomic analysis of breast cancer secretomes. *Cancer Science*, *107*(6), 828–835. https://doi.org/10.1111/cas.12935

Somia, N., & Verma, I. M. (2000). Gene therapy: trials and tribulations. *Nature Reviews. Genetics*, *1*(2), 91–99. https://doi.org/10.1038/35038533

Stolberg, S. G. The biotech death of Jesse Gelsinger. *N Y Times Mag* 136–140, 149–150 (1999).

Thomas, C. E., Ehrhardt, A., & Kay, M. A. (2003). Progress and problems with the use of viral vectors for gene therapy. *Nature Reviews. Genetics*, *4*(5), 346–358. https://doi.org/10.1038/nrg1066

Thomas, C. E., Schiedner, G., Kochanek, S., Castro, M. G., & Löwenstein, P. R. (2000). Peripheral infection with adenovirus causes unexpected long-term brain inflammation in animals injected intracranially with first-generation, but not with high-capacity, adenovirus vectors: toward realistic long-term neurological gene therapy for chronic diseases. *Proceedings of the National Academy of Sciences of the United States of America*, *97*(13), 7482–7487. https://doi.org/10.1073/pnas.120474397

Thomas, C. E., Schiedner, G., Kochanek, S., Castro, M. G., & Lowenstein, P. R. (2001). Preexisting antiadenoviral immunity is not a barrier to efficient and stable transduction of the brain, mediated by novel high-capacity adenovirus vectors. *Human Gene Therapy*, *12*(7), 839–846. https://doi.org/10.1089/104303401750148829

Tropak, M. B., Yonekawa, S., Karumuthil-Melethil, S., Thompson, P., Wakarchuk, W., Gray, S. J., … Mahuran, D. (2016). Construction of a hybrid β-hexosaminidase subunit capable of forming stable homodimers that hydrolyze GM2 ganglioside in vivo. *Molecular Therapy. Methods & Clinical Development*, *3*, 15057. https://doi.org/10.1038/mtm.2015.57

Tropak, M. B., Bukovac, S. W., RIgat, B. A., Yonekawa, S., Wakarchuk, W., & Mahuran, D.J. (2010). A SENSITIVE FLUORESCENCE-BASED ASSAY FOR MONITORING GM2 GANGLIOSIDE HYDROLYSIS IN LIVE PATIENT CELLS AND THEIR LYSATES. *Glycobiology, 20(3), 356-365.* http://doi.org/10.1093/glycob/cwp183

Vandamme, C., Adjali, O., & Mingozzi, F. (2017). Unraveling the Complex Story of Immune Responses to AAV Vectors Trial After Trial. *Human Gene Therapy*, *28*(11), 1061–1074. https://doi.org/10.1089/hum.2017.150

Varki, A. (1993). Biological roles of oligosaccharides: all of the theories are correct. *Glycobiology*, *3*(2), 97–130.

Vitner, E. B., Platt, F. M., & Futerman, A. H. (2010). Common and uncommon pathogenic cascades in lysosomal storage diseases. *The Journal of Biological Chemistry*, *285*(27), 20423–20427. https://doi.org/10.1074/jbc.R110.134452

Wada, R., Tifft, C. J., & Proia, R. L. (2000). Microglial activation precedes acute neurodegeneration in Sandhoff disease and is suppressed by bone marrow transplantation. *Proceedings of the National Academy of Sciences of the United States of America*, *97*(20), 10954–10959.

Walia, J. S., Altaleb, N., Bello, A., Kruck, C., LaFave, M. C., Varshney, G. K., … Triggs-Raine,

B. (2015). Long-term correction of Sandhoff disease following intravenous delivery of rAAV9 to mouse neonates. *Molecular Therapy: The Journal of the American Society of Gene Therapy*, *23*(3), 414–422. https://doi.org/10.1038/mt.2014.240

Wang, P.-R., Xu, M., Toffanin, S., Li, Y., Llovet, J. M., & Russell, D. W. (2012). Induction of hepatocellular carcinoma by in vivo gene targeting. *Proceedings of the National Academy of Sciences of the United States of America*, *109*(28), 11264–11269. https://doi.org/10.1073/pnas.1117032109

Wang, D., Zhong, L., Nahid, M. A. & Gao, G. The potential of adeno-associated viral vectors for gene delivery to muscle tissue. *Expert Opin Drug Deliv* **11**, 345–364 (2014).

Werth, N., Schuette, C. G., Wilkening, G., Lemm, T., & Sandhoff, K. (2001). Degradation of Membrane-bound Ganglioside GM2 by β-Hexosaminidase A STIMULATION BY GM2 ACTIVATOR PROTEIN AND LYSOSOMAL LIPIDS. *Journal of Biological Chemistry*, *276*(16), 12685–12690. https://doi.org/10.1074/jbc.M007970200

Wherrett, J.R., & Cumings, J.N. (1963). Detection and resolution of gangliosides in lipid extracts by thin-layer chromatography. *Biochemical Journal*, 86(2), 378-382.

Wirth, T., Parker, N., & Ylä-Herttuala, S. (2013). History of gene therapy. *Gene*, *525*(2), 162–169. https://doi.org/10.1016/j.gene.2013.03.137

Wright, C. S., Mi, L.-Z., Lee, S., & Rastinejad, F. (2005). Crystal structure analysis of phosphatidylcholine-GM2-activator product complexes: evidence for hydrolase activity. *Biochemistry*, *44*(41), 13510–13521. https://doi.org/10.1021/bi050668w

Xiong, B. *et al.* Precise Cerebral Vascular Atlas in Stereotaxic Coordinates of Whole Mouse Brain. *Front. Neuroanat.* **11**, (2017).

Yanai, H., Yoshida, H., Tomono, Y., Tada, N., & Chiba, H. (2006). The possible contribution of a general glycosphingolipid transporter, GM2 activator protein, to atherosclerosis. *Journal of Atherosclerosis and Thrombosis*, *13*(6), 281–285.

Yang, L. J., Zeller, C. B., Shaper, N. L., Kiso, M., Hasegawa, A., Shapiro, R. E., & Schnaar, R. L. (1996). Gangliosides are neuronal ligands for myelin-associated glycoprotein. *Proceedings of the National Academy of Sciences of the United States of America*, *93*(2), 814–818.

Yuziuk, J. A., Bertoni, C., Beccari, T., Orlacchio, A., Wu, Y. Y., Li, S. C., & Li, Y. T. (1998). Specificity of mouse GM2 activator protein and beta-N-acetylhexosaminidases A and B. Similarities and differences with their human counterparts in the catabolism of GM2. *The Journal of Biological Chemistry*, *273*(1), 66–72.

Zhong, L., Malani, N., Li, M., Brady, T., Xie, J., Bell, P., … Gao, G. (2013). Recombinant adeno-associated virus integration sites in murine liver after ornithine transcarbamylase gene correction. *Human Gene Therapy*, *24*(5), 520–525. https://doi.org/10.1089/hum.2012.112

APPENDIX

Mouse #	Sex	Genotype	Sire	Dam	DOB	Euthanization date
20-week Controls						
82	M	Het	1	26	7/15/2016	12/6/2016
83	M	Het	1	26	7/15/2016	12/6/2016
84	M	Het	1	26	7/15/2016	12/6/2016
85	M	Het	1	26	7/15/2016	12/6/2016
86	F	Het	1	26	7/15/2016	12/6/2016
87	F	Het	1	26	7/15/2016	12/6/2016
20-week AAV-hGM2A (Virus)						
125	M	KO	30	36	8/4/2016	12/15/2016
126	M	KO	30	36	8/4/2016	12/15/2016
127	F	KO	30	36	8/4/2016	10/28/2016
128	F	KO	30	36	8/4/2016	12/16/2016
200	F	KO	52	36	10/24/2016	3/13/2017
201	M	KO	52	36	10/24/2016	3/13/2017
20-week GFP						
140	M	KO	1	58	8/31/2016	1/20/2017

141	M	KO	1	58	8/31/2016	1/20/2017
142	F	KO	1	58	8/31/2016	1/20/2017
143	F	KO	1	58	8/31/2016	1/20/2017
144	M	KO	30	10	9/14/2016	1/20/2017
145	M	KO	30	10	9/14/2016	1/20/2017
20-week Vehicle						
90	M	KO	6	22	7/22/2016	12/9/2016
91	M	KO	6	22	7/22/2016	12/9/2016
92	F	KO	6	22	7/22/2016	12/9/2016
93	F	KO	6	22	7/22/2016	12/9/2016
116	M	KO	2	10	7/31/2016	12/16/2016
117	F	KO	2	10	7/31/2016	12/16/2016
20-week AAV-hGM2A (Adult Virus)						
170	F	KO	52	22	10/1/2016	3/8/2017
172	F	KO	52	22	10/1/2016	3/8/2017
174	F	KO	52	22	10/1/2016	3/8/2017
175	M	KO	52	22	10/1/2016	3/8/2017

176	F	KO	52	22	10/1/2016	3/8/2017
181	M	KO	103	112	10/1/2016	3/8/2017

APPENDIX A. 20-week cohorts which includes respective dams and pups assigned to different groups and survival data included. Dates in red identify those in the cohort that passed away prior to their humane endpoints.

Mouse #	Sex	Genotype	Sire	Dam	DOB	Euthanization date
60-week Controls						
80	M	Het	8	12	7/17/2016	10/5/2017
81	F	Het	8	12	7/17/2016	10/5/2017
104	M	Het	43070	67	7/29/2016	10/5/2017
105	M	Het	43070	67	7/29/2016	10/5/2017
106	M	Het	43070	67	7/29/2016	10/5/2017
107	F	Het	43070	67	7/29/2016	1/16/17
60-week AAV-hGM2A (Virus)						
202	F	KO	52	36	10/24/2016	3/18/2017
203	M	KO	52	36	10/24/2016	01/12/2018
204	M	KO	52	36	10/24/2016	01/12/2018
205	M	KO	52	36	10/24/2016	11/9/16

206	F	KO	52	58	10/27/2016	01/9/2018
207	M	KO	52	58	10/27/2016	01/12/2018
60-week GFP						
146	M	KO	30	10	9/14/2016	11/1/2017
147	M	KO	30	10	9/14/2016	4/7/2017
148	F	KO	52	22	9/10/2016	7/14/2017
149	F	KO	52	22	9/10/2016	11/1/2017
150	F	KO	52	22	9/10/2016	11/1/2017
151	M	KO	52	22	9/10/2016	11/1/2017
60-week Vehicle						
118	F	KO	2	10	7/31/2016	12/16/2016
130	M	KO	30	10	8/24/2016	4/16/2017
131	M	KO	30	10	8/24/2016	11/9/2017
132	M	KO	30	10	8/24/2016	11/9/2017
133	M	KO	30	10	8/24/2016	11/9/2017
134	F	KO	30	10	8/24/2016	2/28/2017
60-week AAV-hGM2A (Adult Virus)						
186	F	KO	52	36	10/2/2016	12/20/2017

187	M	KO	52	36	10/2/2016	09/4/2017
188	F	KO	52	36	10/2/2016	12/20/2017
189	M	KO	52	36	10/2/2016	12/20/2017
190	F	KO	52	36	10/2/2016	12/20/2017
191	M	KO	52	36	10/2/2016	12/20/2017

APPENDIX B. 60-week cohorts which includes respective dams and pups assigned to different groups and survival data included. Dates in red identify those in the cohort that passed away prior to their humane endpoints.